

3-14-2020

Effects of UV-A Light Treatment on Ammonia, Hydrogen Sulfide, Greenhouse Gases, and Ozone in Simulated Poultry Barn Conditions

Myeongseong Lee

Iowa State University and Chungnam National University, leefame@iastate.edu

Jisoo Wi

Iowa State University and Chungnam National University

Jacek A. Koziel

Iowa State University, koziel@iastate.edu

Heekwon Ahn

Iowa State University and Chungnam National University

Peiyang Li

Iowa State University, peiyangl@iastate.edu

See next page for additional authors

Follow this and additional works at: https://lib.dr.iastate.edu/abe_eng_pubs



Part of the [Agriculture Commons](#), [Bioresource and Agricultural Engineering Commons](#), [Environmental Chemistry Commons](#), [Environmental Health Commons](#), and the [Poultry or Avian Science Commons](#)

The complete bibliographic information for this item can be found at https://lib.dr.iastate.edu/abe_eng_pubs/1142. For information on how to cite this item, please visit <http://lib.dr.iastate.edu/howtocite.html>.

This Article is brought to you for free and open access by the Agricultural and Biosystems Engineering at Iowa State University Digital Repository. It has been accepted for inclusion in Agricultural and Biosystems Engineering Publications by an authorized administrator of Iowa State University Digital Repository. For more information, please contact digirep@iastate.edu.

Effects of UV-A Light Treatment on Ammonia, Hydrogen Sulfide, Greenhouse Gases, and Ozone in Simulated Poultry Barn Conditions

Abstract

Gaseous emissions, a side effect of livestock and poultry production, need to be mitigated to improve sustainability. Emissions of ammonia (NH₃), hydrogen sulfide (H₂S), greenhouse gases (GHGs), and odorous volatile organic compounds (VOCs) have a detrimental effect on the environment, climate, and quality of life in rural communities. We are building on previous research to bring advanced oxidation technologies from the lab to the farm. To date, we have shown that ultraviolet A (UV-A) has the potential to mitigate selected odorous gases and GHGs in the context of swine production. Much less research on emissions mitigation has been conducted in the context of poultry production. Thus, the study objective was to investigate whether the UV-A can mitigate NH₃, H₂S, GHGs, and O₃ in the simulated poultry barn environment. The effects of several variables were tested: the presence of photocatalyst, relative humidity, treatment time, and dust accumulation under two different light intensities (facilitated with fluorescent and light-emitting diode, LED, lamps). The results provide evidence that photocatalysis with TiO₂ coating and UV-A light can reduce gas concentrations of NH₃, CO₂, N₂O, and O₃, without a significant effect on H₂S and CH₄. The particular % reduction depends on the presence of photocatalysts, relative humidity (RH), light type (intensity), treatment time, and dust accumulation on the photocatalyst surface. In the case of NH₃, the reduction varied from 2.6–18.7% and was affected by RH and light intensity. The % reduction of NH₃ was the highest at 12% RH and increased with treatment time and light intensity. The % reduction of NH₃ decreased with the accumulation of poultry dust. The % reduction for H₂S had no statistical difference under any experimental conditions. The proposed treatment of NH₃ and H₂S was evaluated for a potential impact on important ambient air quality parameters, the possibility of simultaneously mitigating or generating GHGs. There was no statistically significant change in CH₄ concentrations under any experimental conditions. CO₂ was reduced at 3.8%–4.4%. N₂O and O₃ concentrations were reduced by both direct photolysis and photocatalysis, with the latter having greater % reductions. As much as 6.9–12.2% of the statistically-significant mitigation of N₂O was observed. The % reduction for O₃ ranged from 12.4–48.4%. The results warrant scaling up to a pilot-scale where the technology could be evaluated with economic analyses.

Keywords

air pollution, air quality, poultry, livestock, photocatalysis, photolysis, LED UV, odor, titanium dioxide, emissions

Disciplines

Agriculture | Bioresource and Agricultural Engineering | Environmental Chemistry | Environmental Health | Poultry or Avian Science

Comments

This article is published as Lee, Myeongseong, Jisoo Wi, Jacek A. Koziel, Heekwon Ahn, Peiyang Li, Baitong Chen, Zhanibek Meiirkhanuly, Chumki Banik, and William Jenks. "Effects of UV-A Light Treatment on Ammonia, Hydrogen Sulfide, Greenhouse Gases, and Ozone in Simulated Poultry Barn Conditions." *Atmosphere* 11, no. 3 (2020): 283. DOI: [10.3390/atmos11030283](https://doi.org/10.3390/atmos11030283). Posted with permission.

Creative Commons License









This work is licensed under a [Creative Commons Attribution 4.0 License](https://creativecommons.org/licenses/by/4.0/).

Authors

Myeongseong Lee, Jisoo Wi, Jacek A. Koziel, Heekwon Ahn, Peiyang Li, Baitong Chen, Zhanibek Meiirkhanuly, Chumki Banik, and William S. Jenks

Article

Effects of UV-A Light Treatment on Ammonia, Hydrogen Sulfide, Greenhouse Gases, and Ozone in Simulated Poultry Barn Conditions

Myeongseong Lee ^{1,2} , Jisoo Wi ^{1,2} , Jacek A. Koziel ^{2,*} , Heekwon Ahn ^{1,2}, Peiyang Li ² , Baitong Chen ² , Zhanibek Meiirkhanuly ², Chumki Banik ²  and William Jenks ³

¹ Department of Animal Biosystems Sciences, Chungnam National University, Daejeon 34134, Korea; leefame@iastate.edu (M.L.); jswi@cnu.ac.kr (J.W.); hkahn@cnu.ac.kr (H.A.)

² Department of Agricultural and Biosystems Engineering, Iowa State University, Ames, IA 50011, USA; peiyangl@iastate.edu (P.L.); baitongc@iastate.edu (B.C.); zhanibek@iastate.edu (Z.M.); cbanik@iastate.edu (C.B.)

³ Department of Chemistry, Iowa State University, Ames, IA 50011, USA; wsjenks@iastate.edu

* Correspondence: koziel@iastate.edu; Tel.: +1-515-294-4206

Received: 14 February 2020; Accepted: 9 March 2020; Published: 14 March 2020



Abstract: Gaseous emissions, a side effect of livestock and poultry production, need to be mitigated to improve sustainability. Emissions of ammonia (NH₃), hydrogen sulfide (H₂S), greenhouse gases (GHGs), and odorous volatile organic compounds (VOCs) have a detrimental effect on the environment, climate, and quality of life in rural communities. We are building on previous research to bring advanced oxidation technologies from the lab to the farm. To date, we have shown that ultraviolet A (UV-A) has the potential to mitigate selected odorous gases and GHGs in the context of swine production. Much less research on emissions mitigation has been conducted in the context of poultry production. Thus, the study objective was to investigate whether the UV-A can mitigate NH₃, H₂S, GHGs, and O₃ in the simulated poultry barn environment. The effects of several variables were tested: the presence of photocatalyst, relative humidity, treatment time, and dust accumulation under two different light intensities (facilitated with fluorescent and light-emitting diode, LED, lamps). The results provide evidence that photocatalysis with TiO₂ coating and UV-A light can reduce gas concentrations of NH₃, CO₂, N₂O, and O₃, without a significant effect on H₂S and CH₄. The particular % reduction depends on the presence of photocatalysts, relative humidity (RH), light type (intensity), treatment time, and dust accumulation on the photocatalyst surface. In the case of NH₃, the reduction varied from 2.6–18.7% and was affected by RH and light intensity. The % reduction of NH₃ was the highest at 12% RH and increased with treatment time and light intensity. The % reduction of NH₃ decreased with the accumulation of poultry dust. The % reduction for H₂S had no statistical difference under any experimental conditions. The proposed treatment of NH₃ and H₂S was evaluated for a potential impact on important ambient air quality parameters, the possibility of simultaneously mitigating or generating GHGs. There was no statistically significant change in CH₄ concentrations under any experimental conditions. CO₂ was reduced at 3.8%–4.4%. N₂O and O₃ concentrations were reduced by both direct photolysis and photocatalysis, with the latter having greater % reductions. As much as 6.9–12.2% of the statistically-significant mitigation of N₂O was observed. The % reduction for O₃ ranged from 12.4–48.4%. The results warrant scaling up to a pilot-scale where the technology could be evaluated with economic analyses.

Keywords: air pollution; air quality; poultry; livestock; photocatalysis; photolysis; LED UV; odor; titanium dioxide; emissions

1. Introduction

Gaseous emissions, an unwanted side effect of livestock and poultry production, must be mitigated to improve the sustainability of the industry [1]. This is because the gaseous emissions include various components such as ammonia (NH_3), hydrogen sulfide (H_2S), greenhouse gases (GHGs), and odorous volatile organic compounds (VOCs) that have a detrimental effect on the environment, climate, and quality of life in rural communities [2,3]. Maurer et al. [4] reported on the effectiveness of technologies to reduce gas emissions from livestock and poultry housing, manure storage and treatment, and land application. The maturity and the number of technologies for poultry housing are far below those available for the swine industry [4].

Mitigation technologies can be divided into ‘end-of-pipe’ and ‘source-based’ types [5]. The source-based solution is a method of treating the manure as a source of emissions, such as surficial application of biochar [6], soybean peroxidase [7–9], zeolites and bentonites [10,11], urease inhibitors [12,13], feed additives [14], and manure aeration [15]. The end-of-pipe approach is the physicochemical and biological treatment for mitigating emissions from, for example, barns. Typical examples of the end-of-pipe solution are the use of biofilters [16,17] and scrubbers. Ultraviolet light (UV) can be considered as both end-of-pipe (treating exhaust air from barns) and a source-based (e.g., for improvement of indoor air quality; inside the barn) [1,18–21].

Near-UV (UV-A) irradiative treatment has been evaluated to reduce gas and fine particulate concentrations inside a swine barn as well as for increased feed conversion rates that lower the carbon footprint and improves the sustainability [18]. The ultraviolet range is traditionally broken up into wavelength ranges, labeled A, B, and C, corresponding to progressively shorter and more destructive wavelengths. UV-A (roughly 320–400 nm) is the least toxic of the UV range and is commonly used in commercial indoor tanning and other consumer applications. Treatment can be based on photolysis only (i.e., mitigation primarily via direct absorption UV light) and photocatalysis (i.e., primarily via surface-based reactivity based on the catalyst absorbing the light). Photocatalysis is commonly facilitated with nanoparticulate titanium dioxide (TiO_2), a material that is considered efficient, stable, reasonably durable, and cost-efficient [22–24]. Novel materials for TiO_2 -based photocatalysis can improve the efficiency of photolytic UV-A treatment, as shown in the context of swine production [1,20].

The photocatalysis reaction is initiated when photons of sufficient energy (more than bandgap) irradiates the TiO_2 surface, resulting in electron (e^-)/hole (h^+) generation [23,25,26]. Activation of TiO_2 occurs at wavelengths <400 nm [27]. Although the detailed mechanism of photocatalysis varies with different target pollutants, it is commonly agreed that the primary reactions responsible are interfacial redox reactions of electrons and holes with adsorbed pollutants or mediators such as water [23,28,29].

Gaseous emission treatment in the barn through photocatalysis with TiO_2 and UV-A light has been shown to be effective in reducing NH_3 , GHGs, VOCs, and odor [1,18,19,21] in the context of swine production. However, it is necessary to test whether UV treatment is useful for conditions associated with the poultry barn due to the lack of previous research. In addition, recent advancements in UV, such as novel TiO_2 coatings and energy-efficient UV-A lamps (i.e., light-emitting diode, LED) warrant testing of their applications to poultry housing.

This study was conducted to determine the potential for application of photocatalysis to poultry barn prior to pilot or farm-scale experiments. In other words, the objective of this study was to evaluate the UV-A treatment of NH_3 , H_2S , GHGs, and O_3 in simulated (lab-scale) conditions of a poultry barn. The effects of several variables were tested: (a) treatment time, (b) TiO_2 -based photocatalysis vs. direct photolysis, (c) light intensity (LED vs. fluorescent lamps), (c) poultry dust accumulation on photocatalyst, and (d) relative humidity, RH. Our working hypothesis was that longer treatment time, photocatalysis, LED light, and the presence of moisture, should improve the apparent treatment efficiency, while the presence of dust should not affect it. The experimental NH_3 and H_2S concentrations, treatment times, and RH were selected to provide realistic conditions in poultry barns, and thus to provide useful data for UV-A treatment scaling up. The GHGs and O_3 were measured for a

preliminary assessment of the broader impact of proposed treatment on important ambient and indoor air quality parameters.

2. Methods

2.1. Experimental System

An experimental system to evaluate gas emission reduction efficacy under UV-A irradiation was based on a modified setup from previous research, Figure 1 [21,30]. Three mass flow controllers were used to control the dilution of the standard gases and pure air and the RH. A 500 mL glass gas sampling bulb (Supelco, Bellefonte, PA, USA) was installed before and after the UV treatment reactor. The standard gases flowing through the 200 mL reactor were irradiated with UV-A through a quartz window. The reactor bottom was made from an ordinary glass that was coated with a photocatalyst (nanostructured TiO_2 at $10 \mu\text{g}\cdot\text{cm}^{-2}$ from PureTi, Cincinnati, OH, USA). The reactor temperature was maintained at $25 \pm 3^\circ\text{C}$ while the heat generated by the UV lamps was discharged from the UV chamber by circulating-cooling tubes connected to the isothermal water bath.

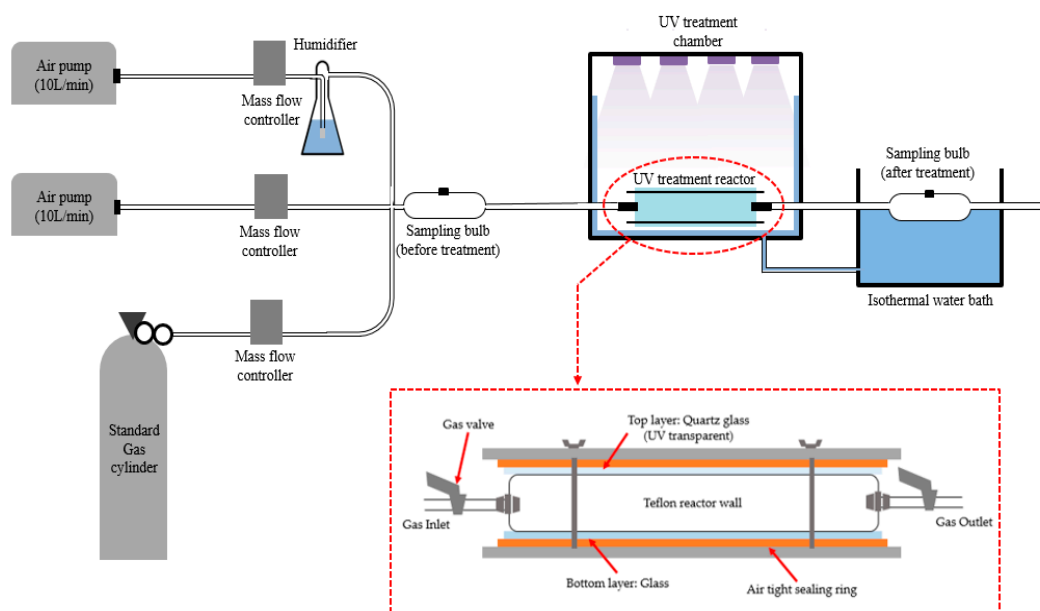




Figure 1. Schematic of UV-based mitigation of target gases at treatment times consistent with scaled-down conditions in the poultry barn.

The gas flow rate into the reactor ranged from $60\text{--}300 \text{ mL}\cdot\text{min}^{-1}$, resulting in a range of 40 s to 200 s treatment time. The treatment time was selected to represent typical air exchange rates inside poultry barns. NH_3 standard gas (70.5 ppm in N_2 , ultra-high-purity, UHP, grade, Praxair, Ames, IA, USA) was diluted to 30 ppm, a typical concentration reported inside poultry barns [31–33]. Similarly, H_2S standard gas (5.2 ppm in N_2 , UHP grade, Praxair) was diluted to 0.5 ppm. The humidifier was used to adjust to three RH levels (approximately 0, 12%, 40%, and 60%). GHGs and O_3 concentrations were measured simultaneously with changes to NH_3 and H_2S . Because ambient air was used as a source, a certain naturally occurring level of GHG and O_3 naturally exists in the background of all experiments in the absence of all treatments. Typical values of NH_3 , H_2S , CH_4 , CO_2 , N_2O , and O_3 were 30 ppm, 0.5 ppm, 2.2 ppm, 350 ppm, 0.2 ppm, and 23 ppb in the absence of any photolytic treatment, i.e., background control runs. The detection methods for each are described below. These environmental parameters were consistent with those observed in typical USA poultry and livestock production barns [34,35]. All experiments were performed in triplicate.

2.2. UV-A Irradiation Sources

Fluorescent lamps (Spectroline, Westbury, NY, USA) and an LED lamp (ONCE, Plymouth, MN, USA) were used; both UV lamps have a primary wavelength of 365 nm (Table 1). The lamps were installed 0.20 m above the UV treatment reactor. The light intensity was measured at 0.20 m distance from the source with an ILT-1700 radiometer equipped with an NS365 filter and SED033 detector (International Light Technologies, Peabody, MA, USA). The LED had $\sim 4\times$ greater intensity compared with the fluorescent lamp for nearly identical power consumption (measured w/ P3 wattage meter, Lexington, NY, USA).

Table 1. Comparison of UV-A lamps.

	Fluorescent	LED
Total light intensity ($\text{mW}\cdot\text{cm}^{-2}$)	0.44	4.85
Power consumption (W)	48.2	43.3
<p>Lamps position inside the UV chamber (4 fluorescent lamps and an array of 108 LED chips on an Al board sources were used)</p> <div style="display: flex; justify-content: space-around;">   </div>		

2.3. Ammonia and Hydrogen Sulfide

NH_3 concentrations were measured in real-time using a Dräger Xam 5600 portable gas analyzer (Luebeck, Germany) with NH_3 sensors (range: 0–300 ppm). The Dräger analyzer was calibrated using Dräger calibration software and standard gases. H_2S was measured (also in real-time) using a gas monitoring system (OMS-300, Smart Control & Sensing Inc., Daejeon, Rep. of Korea) equipped with the $\text{H}_2\text{S}/\text{C}-50$ electrochemical gas sensors from Membrapor Co. (Wallisellen, Switzerland; range: 0–50 ppm). The H_2S gas sensor was calibrated using standard gases. The flow rate used in this study was $60,300 \text{ mL}\cdot\text{min}^{-1}$, NH_3 , and H_2S samples were collected in 5 L Tedlar bags to overcome the limitations associated with the sample collection flow rates required by the portable analyzers (NH_3 : $0.5 \text{ L}\cdot\text{min}^{-1}$ and H_2S : $2 \text{ L}\cdot\text{min}^{-1}$).

2.4. Greenhouse Gases

GHGs samples were collected using syringes by drawing gas from the sampling bulbs and injecting them into evacuated 5.9 mL Exetainer vials (Labco Ltd, UK). Samples were analyzed on a gas chromatography (GC) equipped with a flame ionization detector (FID) and electron capture detector (ECD) detectors (SRI Instruments, Torrance, CA, USA). Standard calibrations were constructed daily using 10.3 ppm and 20.5 ppm CH_4 ; 1,005 ppm and 4,010 ppm CO_2 ; 0.101 ppm and 1.01 ppm N_2O ; and pure helium was used at 0 ppm (Air Liquide America, Plumsteadville, PA, USA) [36]. Samples were stored at 4°C immediately after collection and analyzed within one day after sampling.

2.5. Ozone

A real-time O_3 detector (Gas Sensing, Hull, IA, USA) was connected to the monitoring system (Series 500 monitor, Aeroqual, New Zealand) and installed in the UV treatment chamber. The O_3 concentration was analyzed by measuring the concentration of O_3 collected in a 0.5 L glass gas sampling bulb connected downstream from the UV reactor. The sensor was factory-calibrated before use. The detection range was from 0–0.05 ppm.

2.6. Dust Collection in A Poultry Barn

The presence of accumulated dust could potentially compromise the effectiveness of photocatalyst. Thus, in order to evaluate the effect of dust on mitigation efficiency, dust was collected at Poultry Teaching Farm (Ames, IA, USA). Three Styrofoam boxes that held two glass plates (blank and coated with TiO₂) were placed inside the barn horizontally and accumulated dust over time (Figure 2, part a). Also, three aluminum (Al) foil coupons were attached to simultaneously measure the weight of accumulated dust per area. The Styrofoam boxes were then removed from the barn, one by one, at one-week intervals for three weeks. Then, the same glass plates were mounted into the UV reactor (as the 'Bottom layer: Glass in Figure 1) for testing. The weight of accumulated dust was estimated by subtracting the final from the initial Al foil coupon weight and extrapolated to the entire bottom layer glass area of the reactor. In addition, the effect of accumulated dust on light absorption at the glass with and without TiO₂ was measured using a 300-lumen bulb and a radiometer equipped with an XRD340B detector (International Light Technologies, Peabody, MA, USA), Figure 2 (part b).

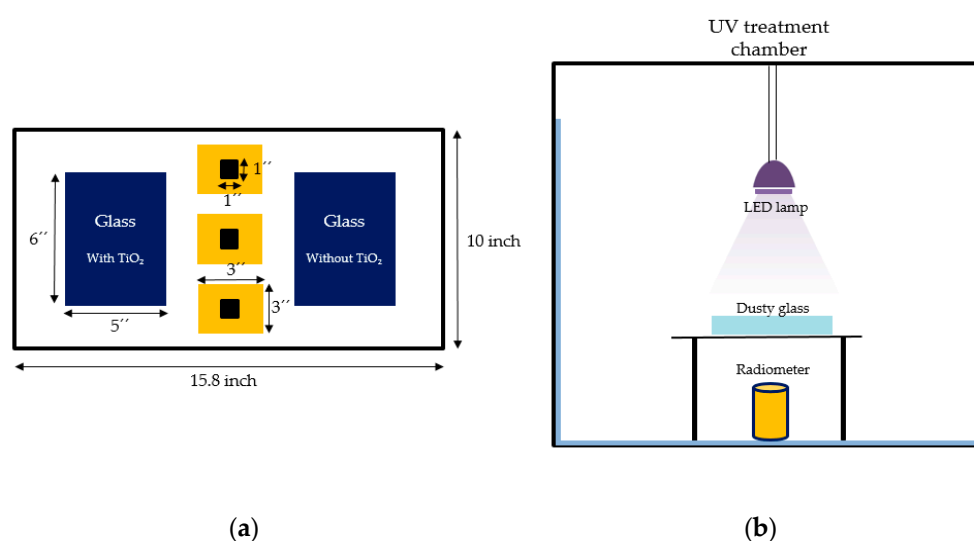


Figure 2. Investigation of the effect of accumulated poultry dust on photocatalysis. (a) Dust collection box; (b) Schematic of the method used for measuring the light absorption by the accumulated dust on the glass (i.e., the bottom layer of the reactor in Figure 1) with and without TiO₂.

2.7. Data analysis, Accounting for Sample Losses Due to Adsorption

Gas samples were collected after a 1 h of equilibration time under each treatment condition. Small, yet consistent losses to target gases were observed over the course of experiments with the photocatalyst. Thus, the standard gas recoveries were also measured and reported as 'adsorption' series in the Results. The adsorption to the photocatalyst was assumed to be responsible for the losses and accounted for in the analyses. The overall mean reduction for each measured gas was estimated using:

$$\% \text{ Reduction} = \frac{C_{Con} - C_{Treat}}{C_{Con}} \times 100\% \quad (1)$$

where: C_{Con} and C_{Treat} are the mean measured concentrations in control and treated air, respectively.

2.8. Statistical Analysis

The R program (version 3.4.2) was used to analyze the effects of the catalyst, lamp-type, and environmental parameters on the reduction of the target gases by one way ANOVA. This statistical analysis generated p -values for evaluating whether a specific parameter/factor had a significant influence on treatment. A significant difference was defined for a p -value < 0.05 .

3. Results

3.1. Ammonia

In general, longer treatment time, use of photocatalyst, increased light intensity, and the presence of moisture in treated air improved the % NH_3 reduction. The highest reduction was 18.7% for 200 s treatment, LED photocatalysis at 12% RH, and no dust conditions. Dust decreased the performance of the photocatalyst. Detailed summaries and statistical significance of the effects of each treatment are presented in the subsections below.

3.1.1. Effect of the Photocatalyst, Relative Humidity, Light Intensity, and Treatment Time

The controlled NH_3 concentration used in the control group using the standard gas was 29.8 ± 1.2 ppm. Figure 3 illustrates the NH_3 reduction at three treatment conditions (direct photolysis, photocatalysis, and adsorption (by TiO_2)) under different RH, and 40 s (part a) and 200 s (part b) treatment time, respectively. Photocatalysis resulted in a 2.6–18.7% reduction, which was statistically significant for nearly all conditions (Tables A1 and A2, Appendix A). In comparison, direct photolysis resulted in no treatment or negligible % reduction and was not statistically significant.

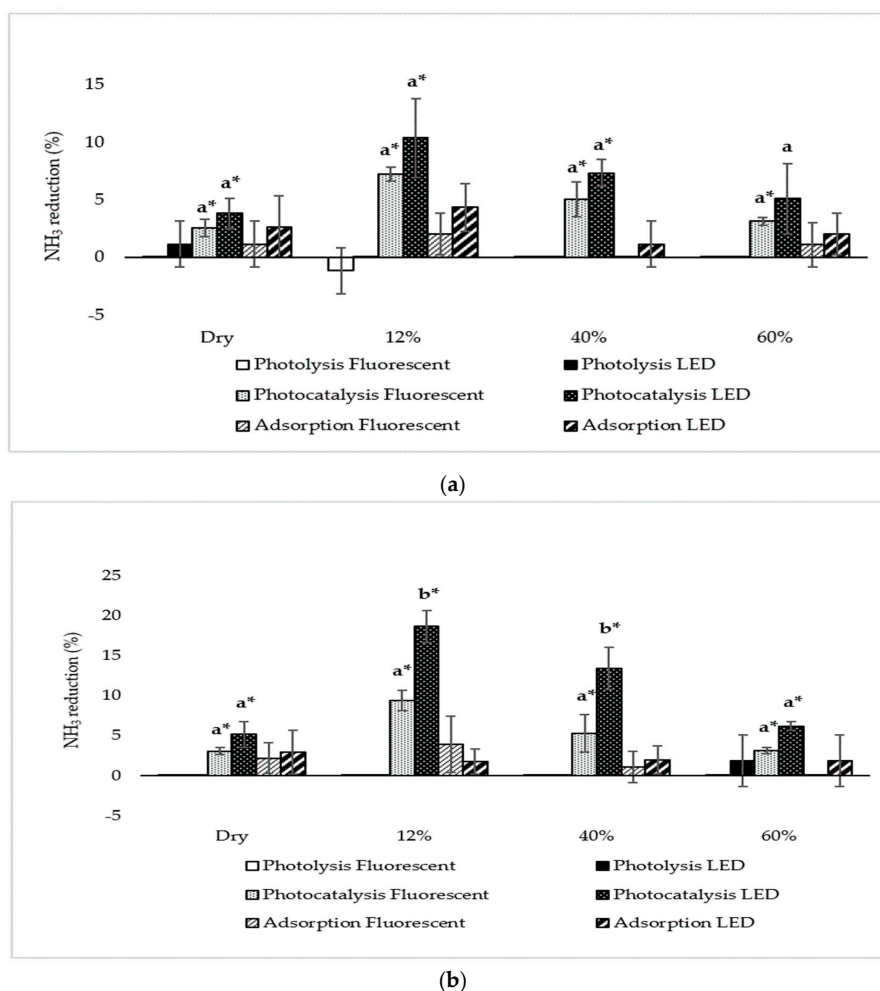


Figure 3. Comparison of NH_3 mitigation under different treatment types and light intensities. (a) % reduction at treatment time of 40 s; (b) % reduction at treatment time of 200 s; Superscript (*) signifies a statistical difference compared to the control ($p < 0.05$), and the different characters (a, b) signify statistical difference when comparing different light intensities (fluorescent vs. LED) at the same relative humidity ($p < 0.05$). The % reduction was the highest at 12% (7.3–18.7%, $p < 0.05$). Error bars signify \pm standard deviation.

Closer inspection of the patterns in the effectiveness of photocatalysis showed that it was affected by RH, light (type) intensity, and treatment time. The LED lamp (having $\sim 4\times$ higher intensity) facilitated a higher % reduction, the greatest ($\sim 2\times$) improvement observed at 12% RH. Moreover, the statistical difference in this improvement was shown for both RH 12% and 40% at 200 s treatment (Figure 3, part b).

Figure 4 highlights the % reduction with different treatment times and RH. The LED-based photocatalysis at lower RH (12% and 40%) outperformed the fluorescent-based treatment for NH_3 mitigation.

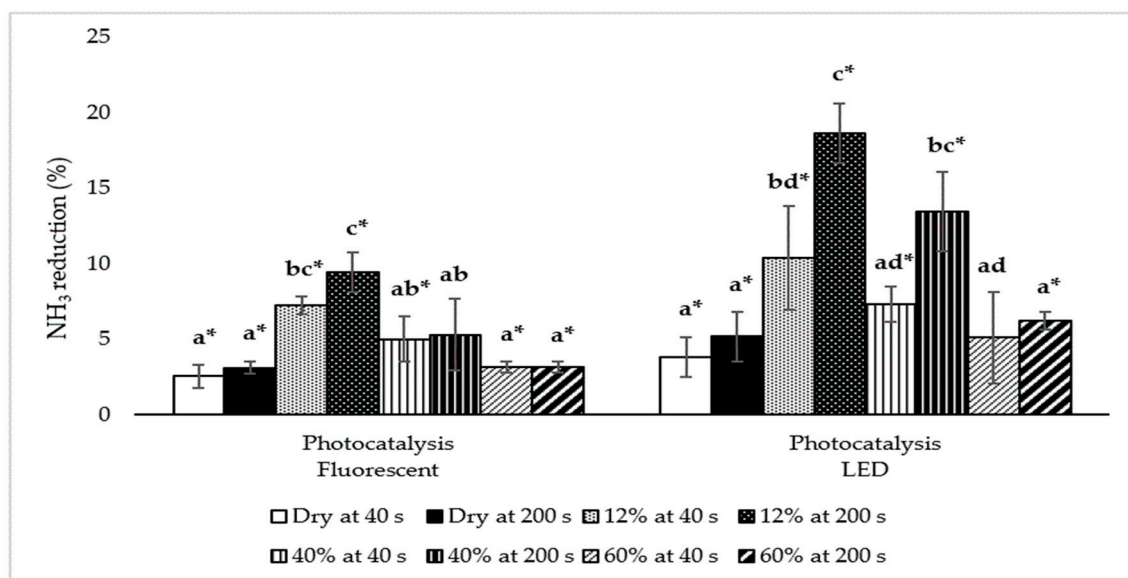


Figure 4. Comparison of NH_3 mitigation under different relative humidity and treatment time. Superscript (*) signifies a statistical difference compared to the control ($p < 0.05$), and the different characters (a, b, c, d) signify the statistical difference between treatments associated with one UV lamp type ($p < 0.05$). Error bars signify \pm standard deviation.

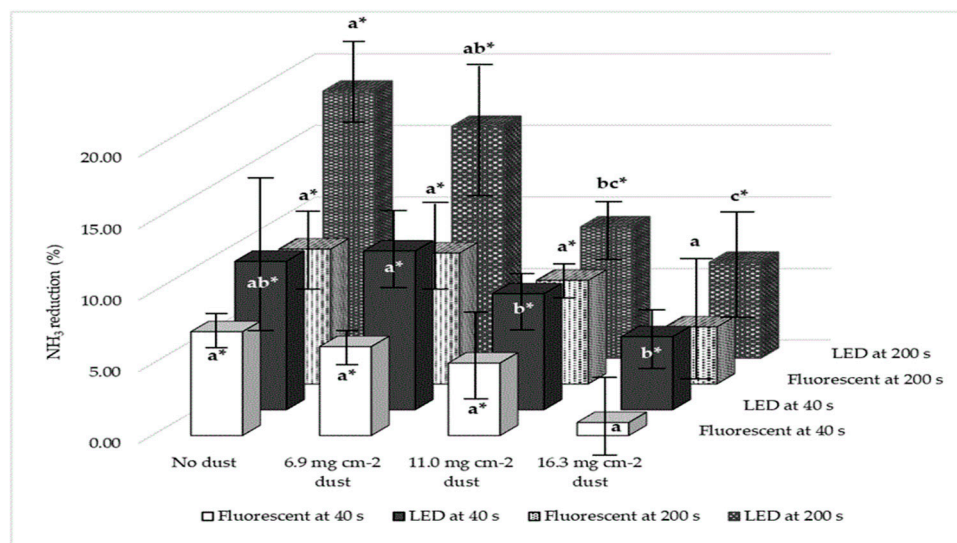
3.1.2. Effect of Poultry Dust

Dust accumulation on TiO_2 had a detrimental effect on the effectiveness of photocatalysis (Figure 5, Tables A3 and A4), particularly at low RH (12%). In addition, accumulated poultry dust absorbed light, and the linear increase (from 14.1 to 40.1%) in light absorption with dust accumulation on the photocatalyst surface over time (from 6.9 to 16.3 $\text{mg}\cdot\text{cm}^{-2}$) was observed. The average light absorption was $27 \pm 12\%$, and the dust accumulation was $11 \pm 4 \text{ mg}\cdot\text{cm}^{-2}$ (Table 2).

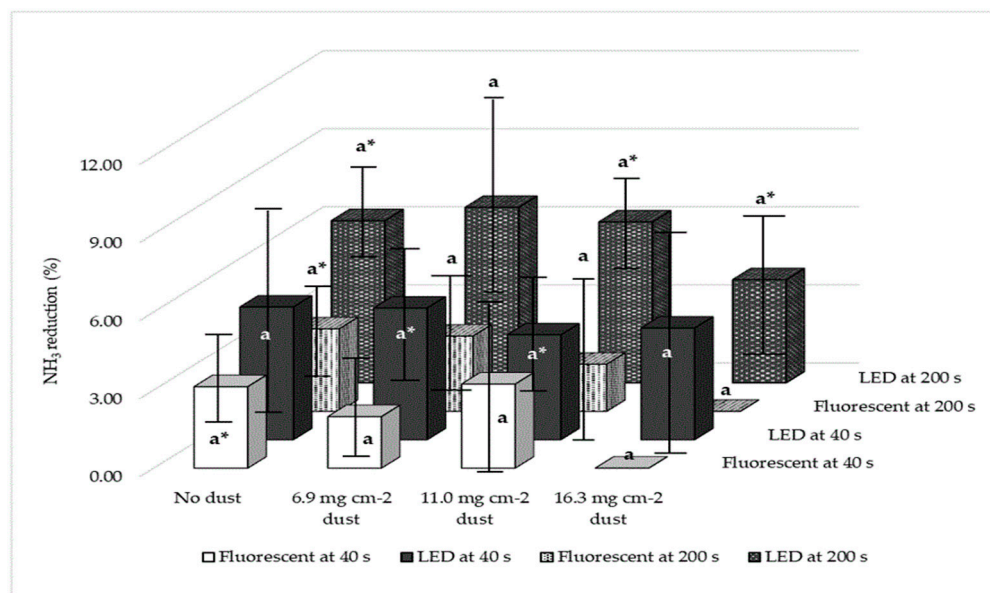
Table 2. Light absorption by accumulated dust and weight of accumulated poultry dust on TiO_2 .

Dust Accumulation Duration	Light Absorption (%)	Dust Accumulation ($\text{mg}\cdot\text{cm}^{-2}$)
1 week	14.1 ± 3.6	6.9 ± 0.4
2 weeks	27.1 ± 4.0	11.0 ± 0.7
3 weeks	40.1 ± 5.9	16.3 ± 1.3
Average	27.1 ± 12	11.4 ± 4.2

The values in the table report the mean \pm standard deviation.



(a)



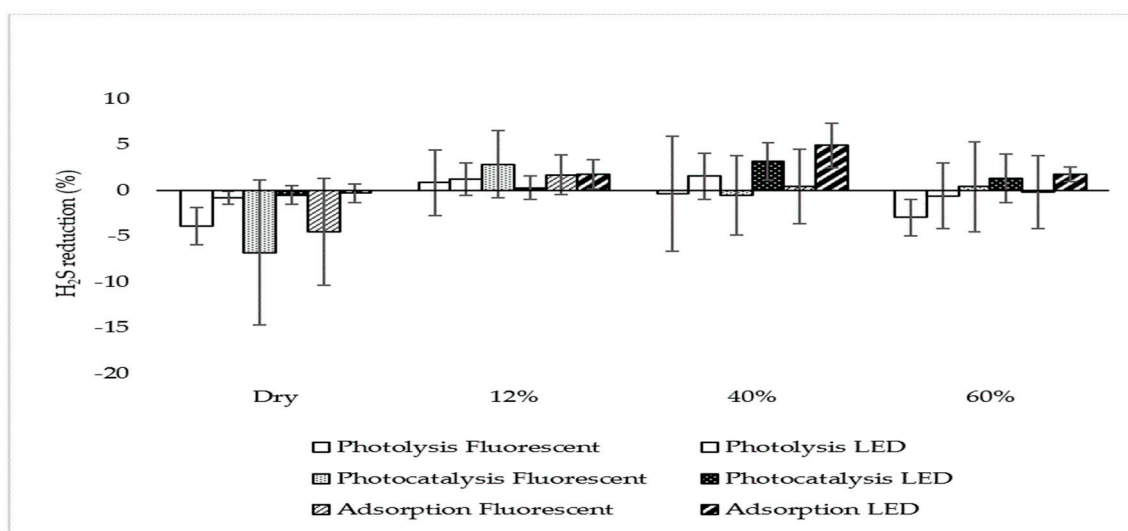
(b)

Figure 5. Comparison of NH_3 mitigation under different poultry dust levels. (a) % reduction at relative humidity of 12%; (b) % reduction at relative humidity of 60%; Superscript (*) signifies a statistical difference compared to the control ($p < 0.05$), and the different characters (a, b, c) signify statistical difference at the same treatment time and the same light intensity ($p < 0.05$). Error bars signify \pm standard deviation.

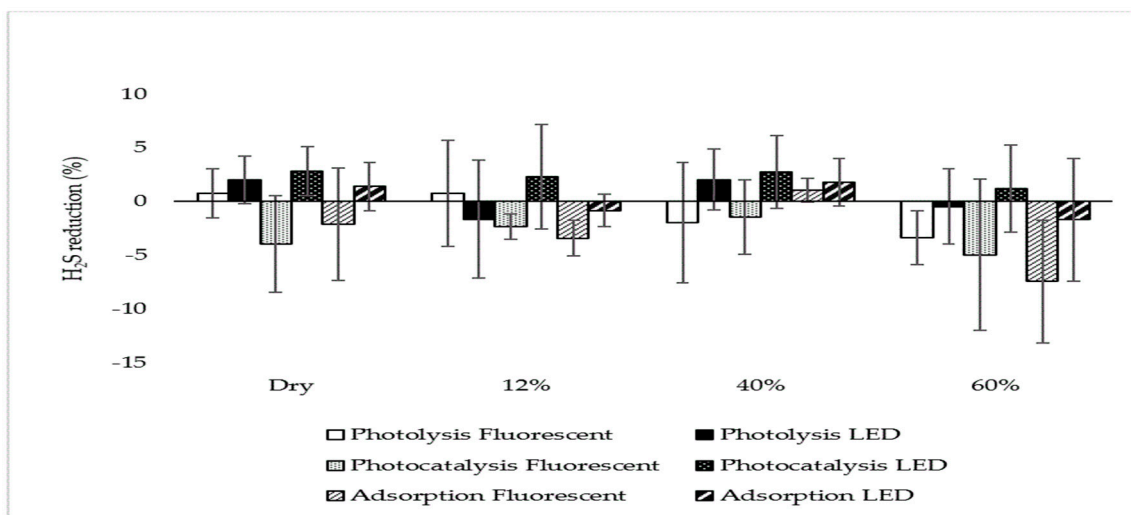
There was no statistical significance of the change in the reduction at RH 60% (Figure 5, part b). The low (12%) RH had the most considerable decrease in mitigation (from 18.7% to 5.1%) under the LED light, yet it was still statistically significant even with the highest dust accumulation of 16.3 mg·cm⁻² ($p < 0.05$). In other words, the LED-based treatment was still performing well, regardless of dust accumulation ($p < 0.05$).

3.2. Hydrogen Sulfide

The controlled H_2S concentration in the control group using the standard gas was 0.52 ± 0.02 ppm. No statistically significant reduction in H_2S concentration was observed under any experimental conditions ($p > 0.05$), even with the most favorable conditions of 200 s, photocatalyst usage, LED irradiation, and elevated moisture (Figure 6). Similarly, there was no statistical difference associated with the dust accumulation at 12% RH regardless of the light type (intensity) and treatment time (Figure 7).



(a)



(b)

Figure 6. Comparison of H_2S mitigation under relative humidity. (a) % reduction at a treatment time of 40 s; (b) % reduction at a treatment time of 200 s. Error bars signify \pm standard deviation.

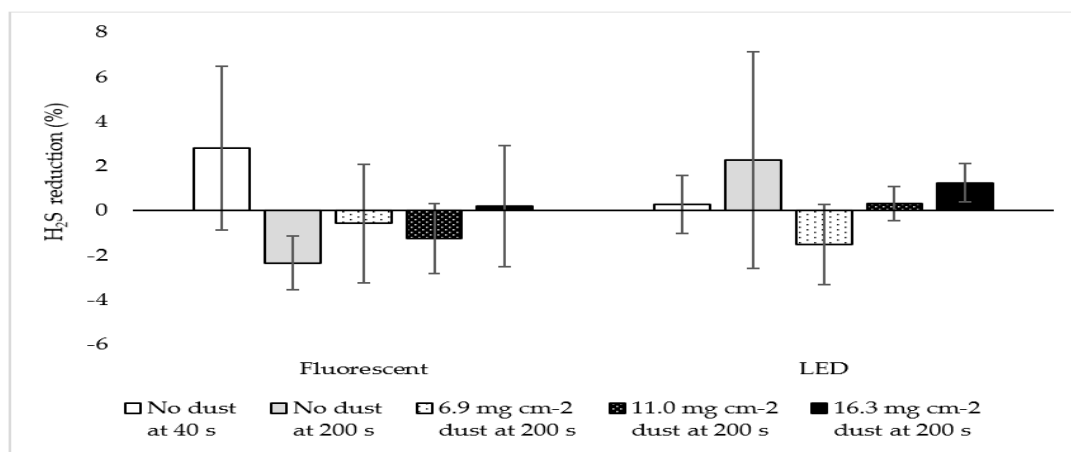


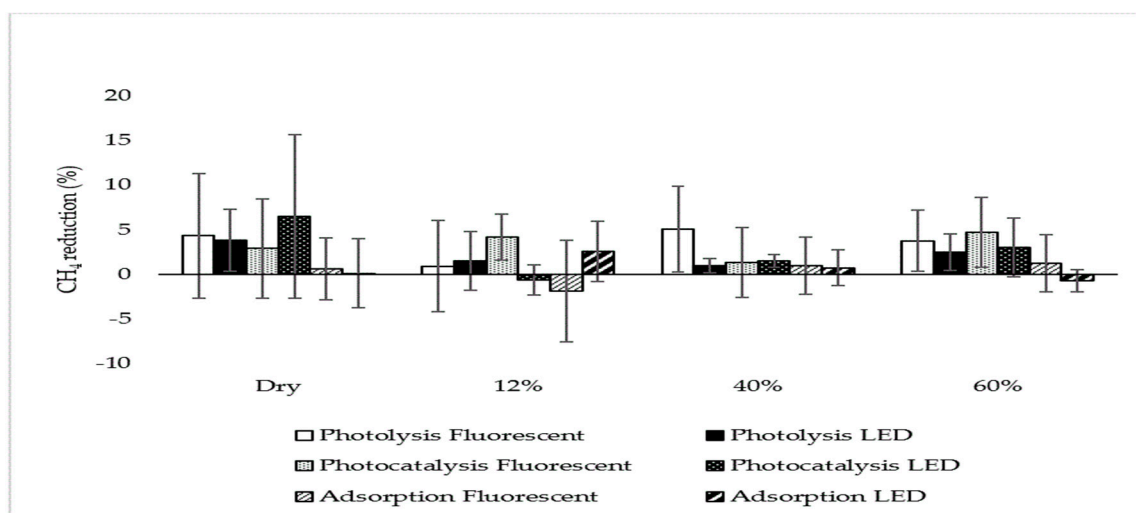
Figure 7. H₂S mitigation under different poultry dust levels at 12% of relative humidity in photocatalysis. Error bars signify \pm standard deviation.

3.3. Greenhouse Gases

The treatment of target gases (NH₃, H₂S) was evaluated for a potential impact on important ambient air quality parameters, the possibility of simultaneously mitigating or generating GHGs. No GHGs were fed into the reactor; however, as noted previously, the air source naturally contained measurable amounts of these compounds. Thus, the GHGs concentrations in the treatment and control were compared.

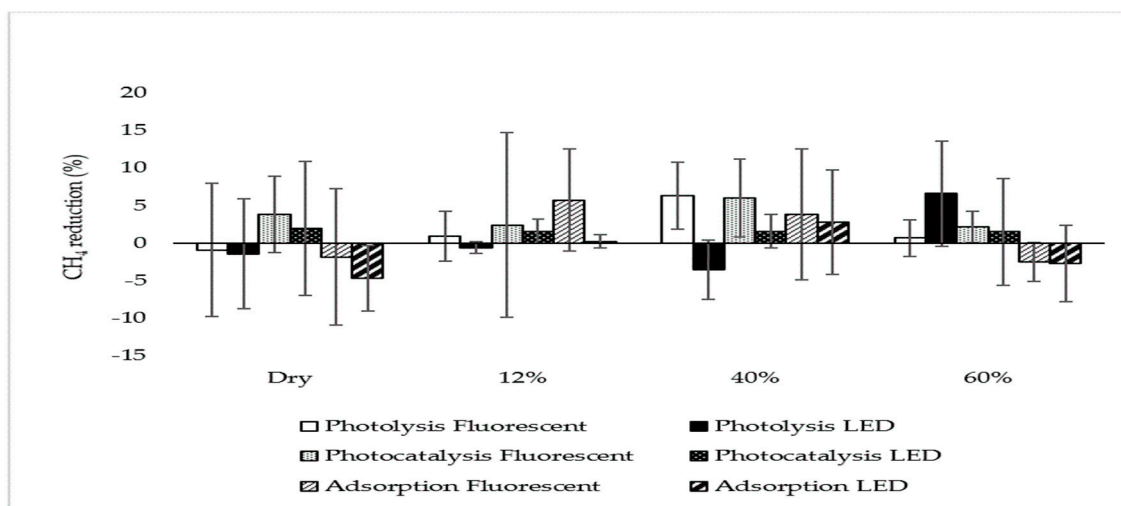
3.3.1. Methane

The average concentration in controls was 2.2 ± 0.1 ppm. There was no statistically significant change in CH₄ concentration under direct photolysis, photocatalysis, and adsorption to the catalyst. Moreover, there were no statistically significant changes, regardless of RH, light type (intensity), treatment time, and dust accumulation when NH₃ and H₂S standard gases were treated with UV (Figures 8 and 9).



(a)

Figure 8. Cont.



(b)

Figure 8. Comparison of CH₄ mitigation under relative humidity. (a) % reduction at a treatment time of 40 s; (b) % reduction at a treatment time of 200 s. Error bars signify \pm standard deviation.

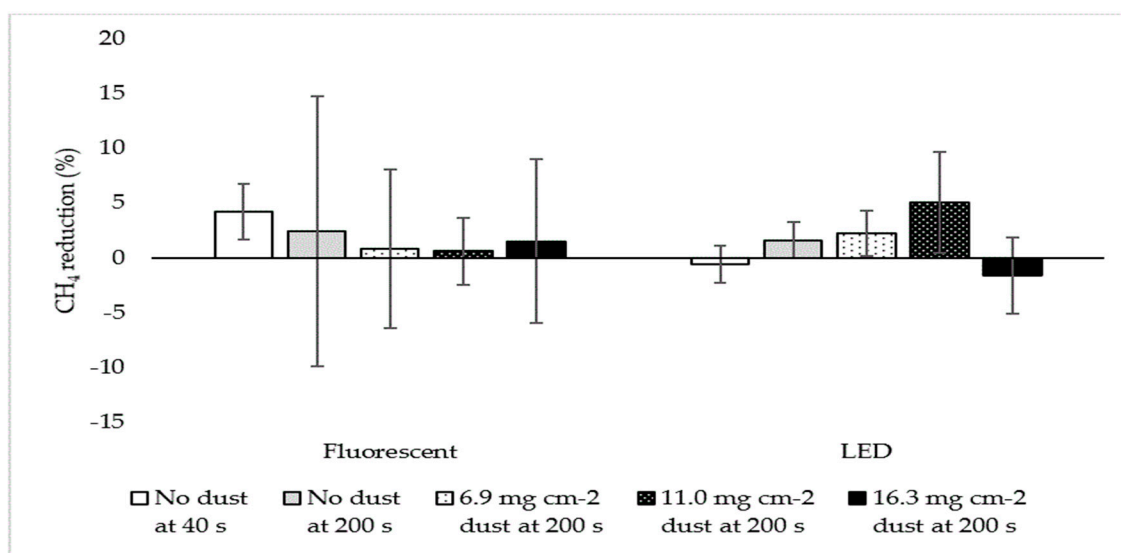


Figure 9. CH₄ mitigation under different poultry dust levels at 12% relative humidity in photocatalysis. Error bars signify \pm standard deviation.

3.3.2. Carbon Dioxide

The average CO₂ concentration in control samples (i.e., present naturally in air) was 350 ± 25 ppm, and no mitigation was observed under photolysis and adsorption. Interestingly, there was a 3.8% (mean) reduction at 200 s photocatalysis with LED at 12% RH (Figure 10 and Table A5). Specifically, the mitigation was 3.2% and 4.4% when NH₃ and H₂S standard gases were treated, respectively. However, there was no statistical difference between the two standard gases ($p > 0.05$). There was no CO₂ reduction under dust accumulation (Figure 11).

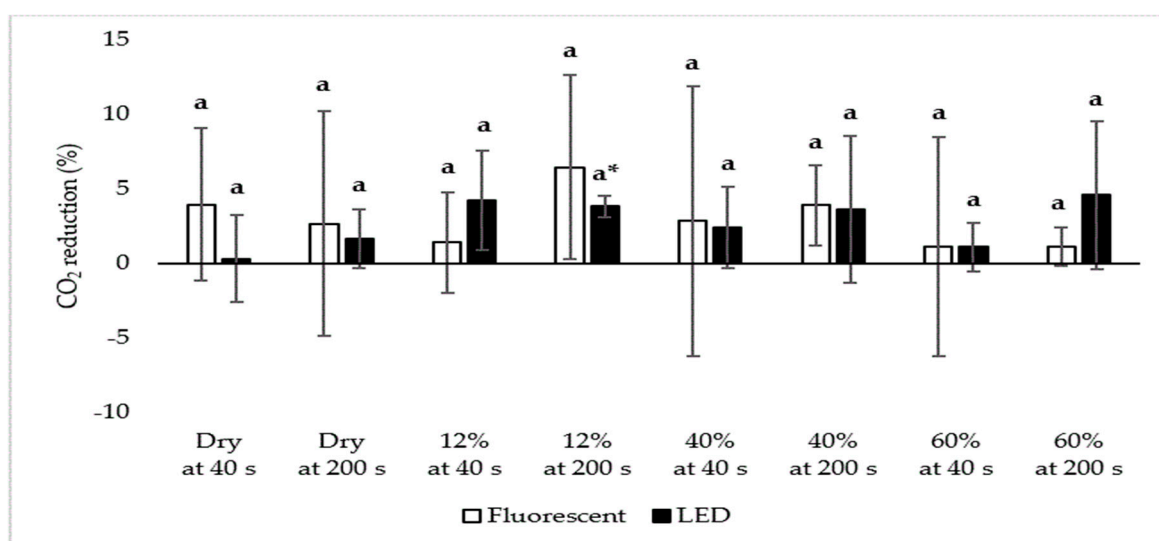


Figure 10. CO₂ mitigation under different light intensity, treatment time, and relative humidity in photocatalysis. Superscript (*) signifies a statistical difference compared to the control ($p < 0.05$), and the character (a) signifies there is no statistical difference under the two different treatment times ($p > 0.05$). Error bars signify \pm standard deviation.

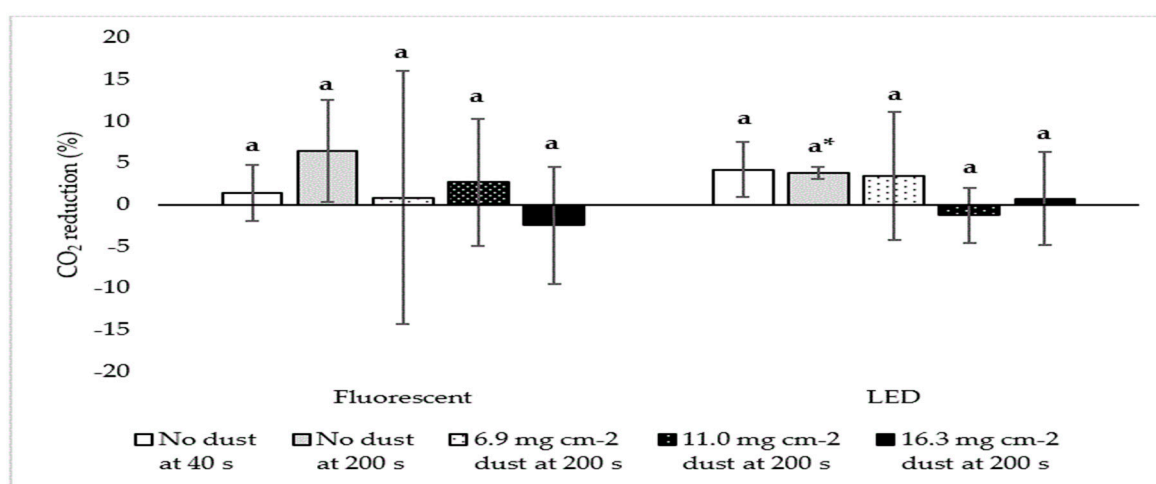


Figure 11. CO₂ mitigation under different poultry dust levels at 12% of relative humidity in photocatalysis. Superscript (*) signifies a statistical difference compared to the control ($p < 0.05$), and the character (a) signifies there is no statistical difference under the two different treatment times ($p > 0.05$). Error bars signify \pm standard deviation.

3.3.3. Nitrous Oxide

In general, mitigation of concentration was observed under both direct photolysis and photocatalysis, with greater reductions with TiO₂ photocatalysts. However, there was no statistical difference between the two conditions. There was no apparent relationship between N₂O % reduction and other controlled parameters.

Comparison of N₂O Mitigation when Treating NH₃ and H₂S Standard Gas

The average N₂O concentration in control was 0.24 ± 0.03 ppm. As much as 6.9% and 12.2% of the statistically-significant % reduction were observed for 200 s photocatalysis with LED at 12% RH when NH₃ and H₂S were treated, respectively (Table 3). In general, statistically-significant % reductions were found for more experimental conditions for H₂S than NH₃. However, there was no significant

difference between the % reduction resulting from the use of two standard gas treatments (i.e., *p*-values in Table 3).

Table 3. The mitigation of N₂O during photocatalysis of NH₃ and H₂S standard gases.

Relative Humidity	Type of UV Lamp	40 s Treatment Time			200 s Treatment Time		
		Standard Gas		<i>p</i> -Value ¹	Standard Gas		<i>p</i> -Value ¹
		NH ₃	H ₂ S		NH ₃	H ₂ S	
Dry	Fluorescent LED	4.1 ± 8.2	5.6 ± 1.3	0.83	2.7 ± 1.7	4.6 ± 0.0 *	0.36
		5.1 ± 3.2	7.9 ± 0.5 *	0.95	4.2 ± 0.0 *	5.9 ± 0.2 *	0.49
12%	Fluorescent LED	3.0 ± 4.1	3.1 ± 2.8	0.44	1.8 ± 2.1	4.8 ± 0.4 *	0.69
		6.2 ± 4.0	11.7 ± 5.9	0.09	6.8 ± 1.6 *	12.2 ± 1.0 *	0.05
40%	Fluorescent LED	3.4 ± 0.3 *	3.3 ± 0.1 *	0.53	1.5 ± 1.0	4.5 ± 2.3	0.49
		5.5 ± 1.1 *	6.8 ± 1.7 *	0.33	8.6 ± 3.1	11.6 ± 8.9	0.09
60%	Fluorescent LED	2.4 ± 0.6	3.3 ± 0.5 *	0.94	5.8 ± 6.5	5.4 ± 0.3	0.12
		4.0 ± 1.8	6.3 ± 5.1	0.85	5.3 ± 1.4	4.7 ± 0.5 *	0.78

The value in the table reports the mean ± standard deviation. Superscript (¹) signifies value from the statistical analysis of the N₂O concentrations reduced under the two standard gases. Superscript (*) signifies a statistical difference compared to the control (*p* < 0.05).

Effect of Photocatalyst, Light Type, Relative Humidity, Dust, and Treatment Time on N₂O

We further investigated the apparent mitigation of N₂O (a potent GHGs) by averaging the results for H₂S and NH₃ to elucidate possible mechanisms responsible for this finding. The statistically significant mitigation was observed in both direct photolysis and photocatalysis, at 3.3–6.5% and 2.8–9.5%, respectively (Figure 12, Tables A6 and A7). In general, photocatalysis was more effective for reducing N₂O than photolysis alone (Figure 12, parts a and b, Tables A6 and A7). However, there was no statistical difference between the two treatments (i.e., at dry and 12% RH, Table A7) were compared. Similarly, no apparent statistical significance was found for variation of the treatment time, dust accumulation, lamp type, and RH (Figures 13 and 14, Tables A8–A10). This is because there are few statistically significant % reduction of N₂O for variable parameters, without any apparent trend.

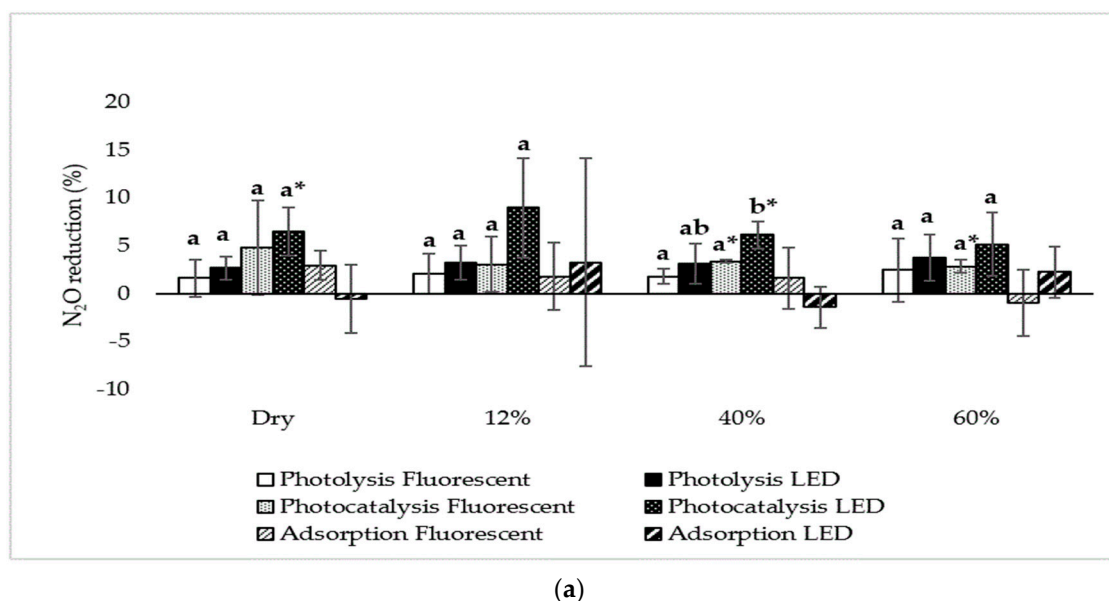
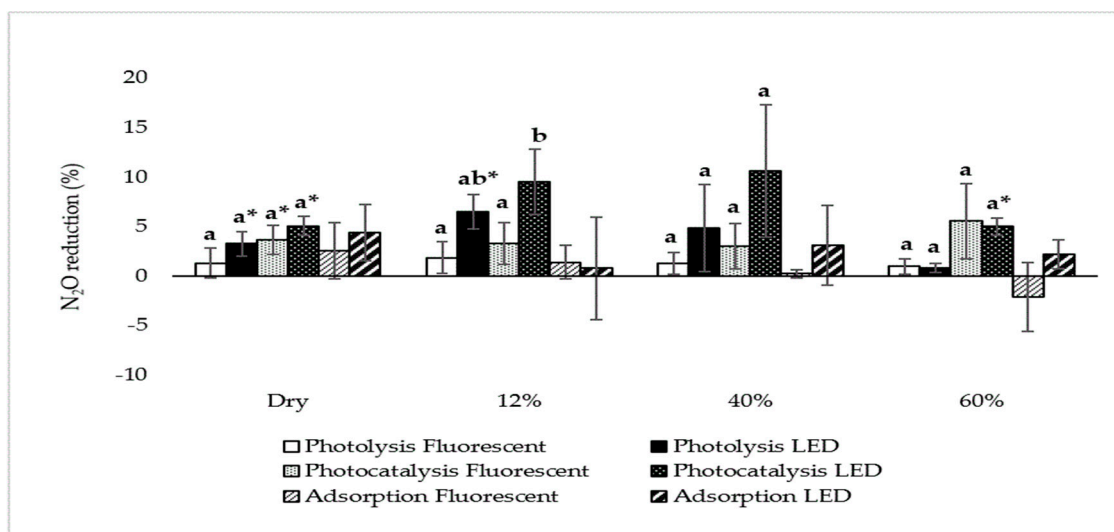


Figure 12. Cont.



(b)

Figure 12. Comparison of N₂O mitigation under different treatment types and light type intensity. (a) % reduction at treatment time of 40 s; (b) % reduction at treatment time of 200 s; Superscript (*) signifies a statistical difference compared to the control ($p < 0.05$), and the different characters (a, b) signify statistical difference when comparing different light intensities (fluorescent vs. LED) at the same relative humidity ($p < 0.05$). Error bars signify \pm standard deviation.

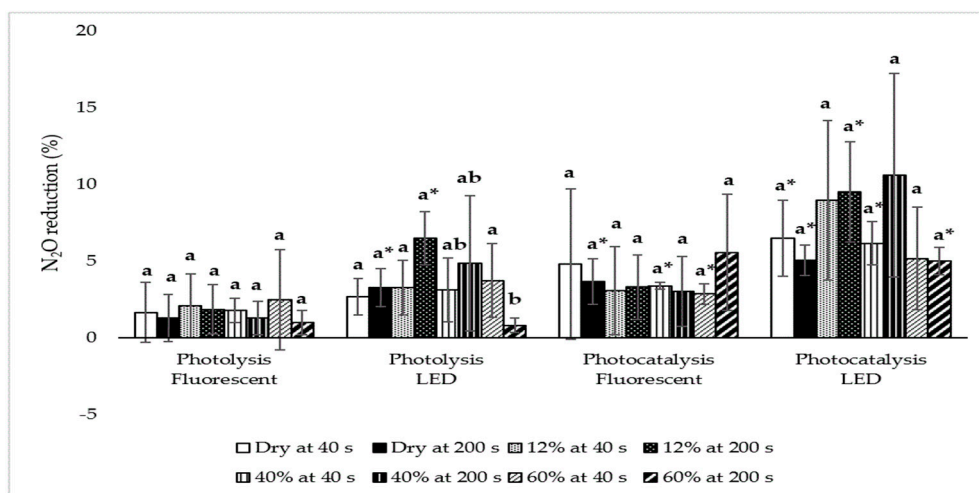
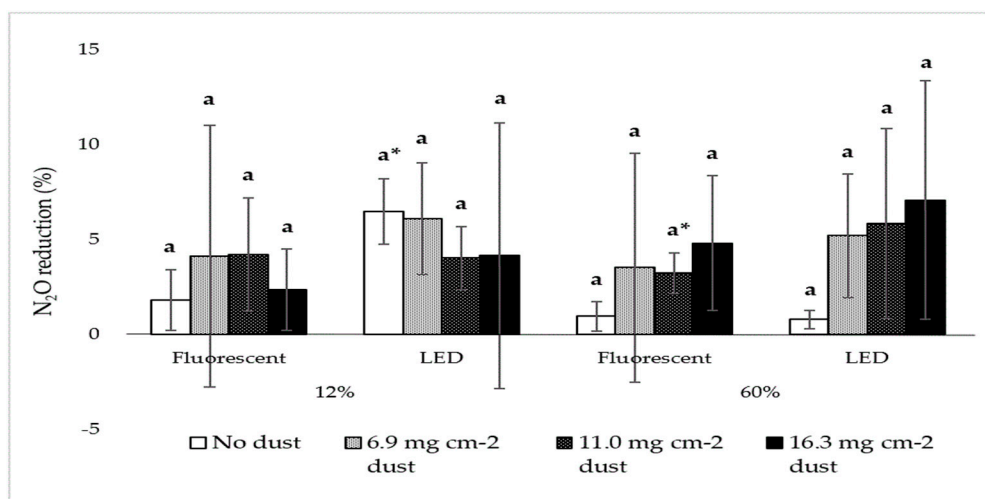
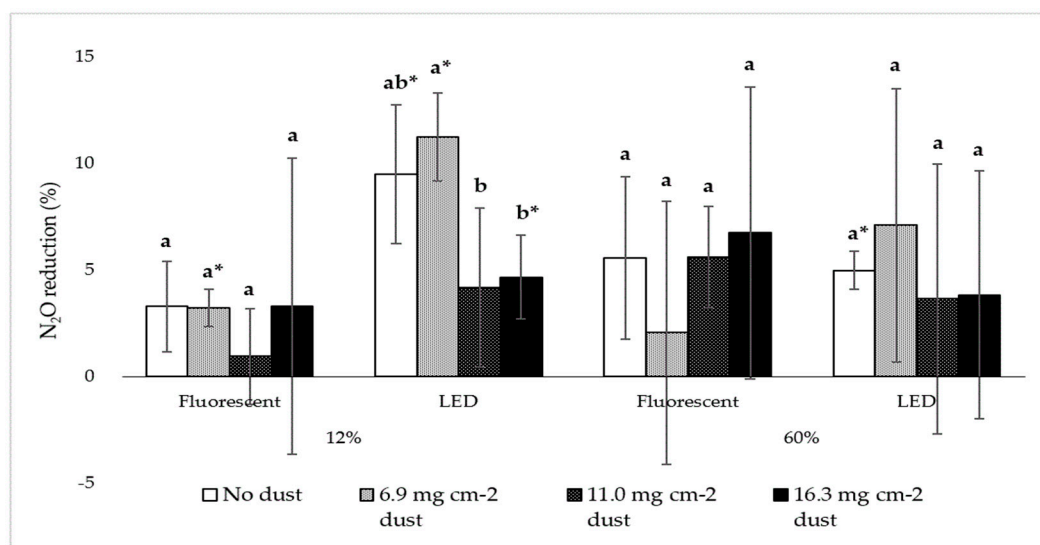


Figure 13. Comparison of N₂O mitigation under different relative humidity and treatment time. Superscript (*) signifies a statistical difference compared to the control ($p < 0.05$), and the different characters (a, b) signify the statistical difference between treatments associated with one UV lamp type ($p < 0.05$). Error bars signify \pm standard deviation.



(a)



(b)

Figure 14. Comparison of N₂O mitigation under different poultry dust levels at 200 s of treatment time. (a) % reduction at a relative humidity of 12% and 60% in direct photolysis; (b) % reduction at a relative humidity of 12% and 60% in photocatalysis. Superscript (*) signifies a statistical difference compared to the control ($p < 0.05$), and the different characters (a, b) signify the statistical difference between treatments associated with one UV lamp type and one relative humidity ($p < 0.05$). Error bars signify \pm standard deviation.

3.4. Ozone

Concerns about O₃ generation when UV light is used were addressed in this research. In general, O₃ concentrations were significantly reduced under direct photolysis and photocatalysis. The direct photolysis treatment did not result in a clear relationship between the controlled parameters and the O₃ % reduction. Photocatalysis resulted in an improved mitigation dependent on the light type (intensity) at RH of 12% and 60%. However, there was no effect associated with treatment time and dust accumulation.

3.4.1. Comparison of Mitigation under NH₃ and H₂S Standard Gas

The average concentration of O₃ in the control group was 22.6 ± 6.5 ppb. As much as 46.5% & 50.3% of the statistically-significant % reduction in O₃ concentrations were observed for 200 s photocatalysis with LED at 12% RH when NH₃ and H₂S were treated, respectively (Table 4). However, there was no significant difference between the reduction resulting from the use of two standard gas treatments (i.e., *p*-values, Table 4). In addition, a statistically significant % reduction was found at more experimental conditions under 200 s treatment time compared with 40 s.

Table 4. The mitigation of O₃ at photocatalysis under NH₃ and H₂S standard gas.

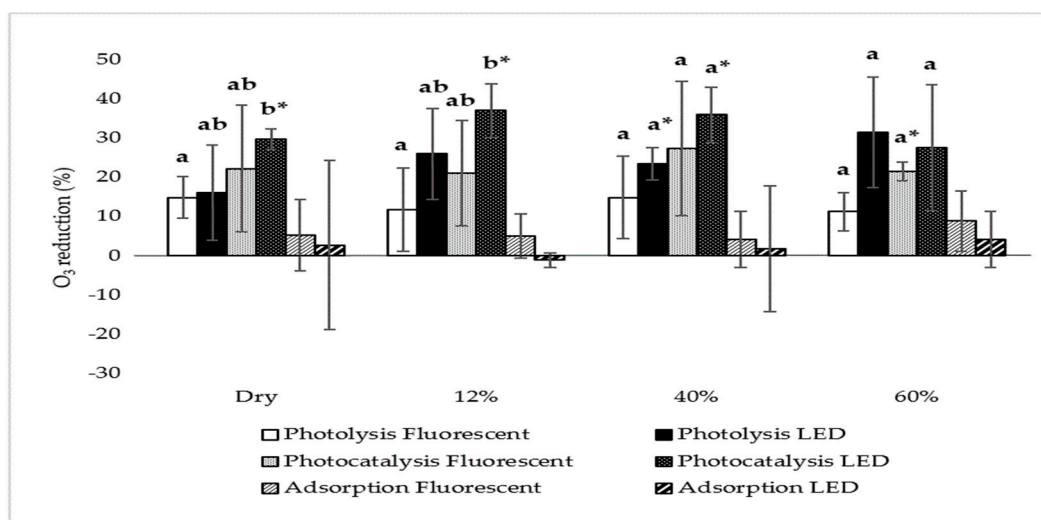
Relative Humidity	Type of UV Lamp	40 s Treatment Time			200 s Treatment Time		
		Standard Gas		<i>p</i> -Value ¹	Standard Gas		<i>p</i> -Value ¹
		NH ₃	H ₂ S		NH ₃	H ₂ S	
Dry	Fluorescent LED	33.5 ± 15.4	11.0 ± 6.8	0.22	27.1 ± 2.1 *	18.0 ± 0.2 *	0.13
		28.4 ± 3.3 *	31.0 ± 1.6 *	0.50	31.7 ± 2.3 *	25.7 ± 0.5 *	0.16
12%	Fluorescent LED	22.0 ± 17.6	20.3 ± 15.1	0.38	24.4 ± 0.9 *	23.0 ± 4.2	0.27
		39.3 ± 10.4	34.7 ± 3.5 *	0.37	50.3 ± 2.4 *	46.5 ± 8.0 *	0.89
40%	Fluorescent LED	34.6 ± 24.0	20.2 ± 9.7	0.67	22.3 ± 0.5 *	21.2 ± 9.0 *	0.57
		40.6 ± 4.4 *	31.4 ± 6.7	0.48	29.7 ± 5.2 *	22.4 ± 0.7 *	0.46
60%	Fluorescent LED	23.2 ± 2.5 *	20.0 ± 0.5 *	0.69	23.4 ± 1.2 *	23.8 ± 0.0 *	0.40
		26.1 ± 21.2	29.1 ± 17.5	0.50	41.8 ± 0.6 *	33.3 ± 2.5 *	0.06

Values in the table report the mean ± standard deviation. Superscript (¹) signifies value from the statistical analysis of the N₂O concentrations reduced under the two standard gases. Superscript (*) means there is a statistical difference compared to the control (*p* < 0.05).

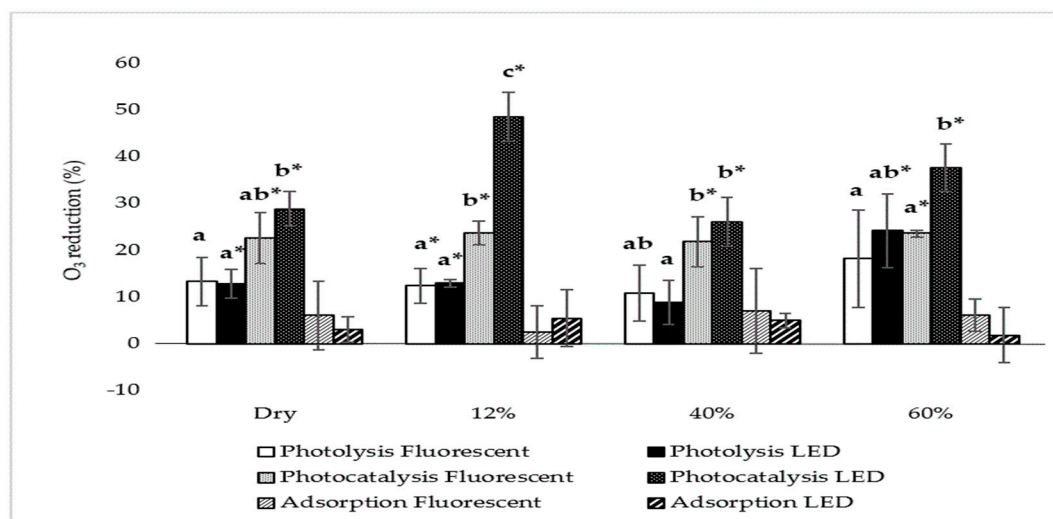
3.4.2. Effect of Photocatalyst, Light Type, Relative Humidity, Dust, and Treatment Time on O₃

O₃ % reduction for various parameters was evaluated using the average of % reductions for treatments of NH₃ and H₂S standard gases. There was significant mitigation on direct photolysis and photocatalysis of 12.4–23.5% and 21.6–48.4%, respectively (Figure 15, Tables A11 and A12). In general, photocatalysis was more effective for reducing O₃ concentrations than was direct photolysis. However, there was no statistical difference between the direct photolysis and photocatalysis except the condition of 200 s at dry and 12% RH (Figure 15, part b). Notably, the % reduction increased ~4× for 200 s photocatalysis with LED at 12% RH (Table A12).

In the case of direct photolysis, there was no clear trend and statistical significance for the treatment time, dust accumulation, lamp type, and RH (Figures 15–17, Tables A11–A14). More statistically-significant % reductions were found for 200 s treatments than 40 s. Moreover, even the maximum accumulation of dust did not have a significant impact on % reduction (Figure 17, Tables A15 and A16).



(a)



(b)

Figure 15. Comparison of O_3 mitigation under different treatment types and light intensity. (a) % reduction at treatment time of 40 s; (b) % reduction at treatment time of 200 s; Superscript (*) signifies a statistical difference compared to the control ($p < 0.05$), and the different characters (a, b) signify a statistical difference when comparing different light intensities (fluorescent vs. LED) at the same relative humidity ($p < 0.05$). Error bars signify \pm standard deviation.

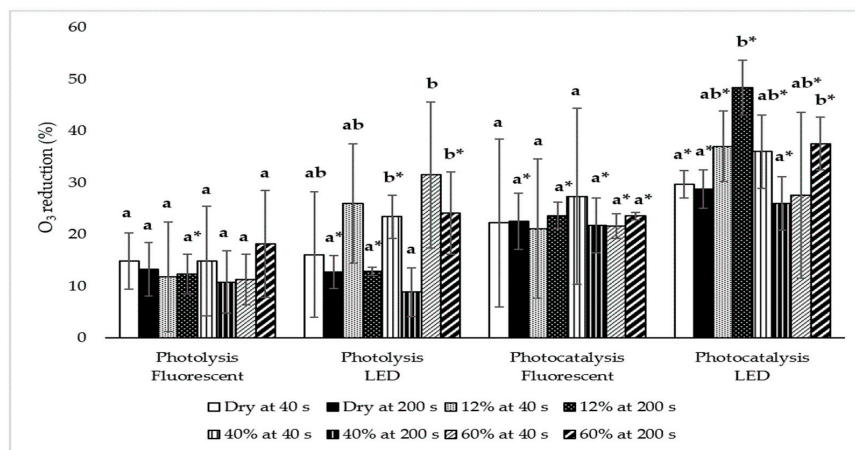
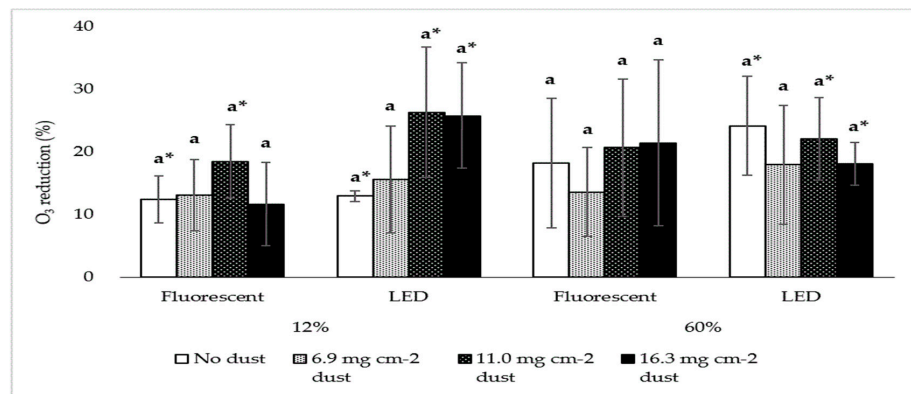
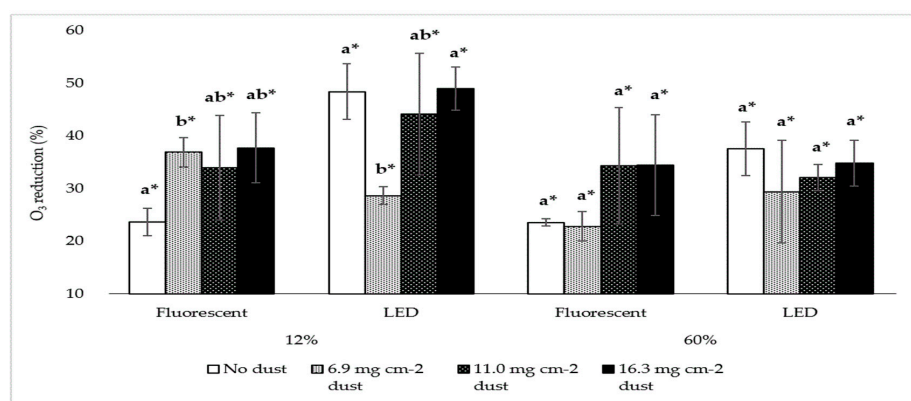


Figure 16. Comparison of O_3 mitigation under different relative humidity and treatment time. Superscript (*) signifies a statistical difference compared to the control ($p < 0.05$), and the different characters (a, b) signify a statistical difference between treatments associated with a lamp type ($p < 0.05$). Error bars signify \pm standard deviation.



(a)



(b)

Figure 17. Comparison of O_3 mitigation under different poultry dust levels. (a) % reduction at a relative humidity of 12% and 60% in direct photolysis; (b) % reduction at a relative humidity of 12% and 60% in photocatalysis. Superscript (*) signifies a statistical difference compared to the control ($p < 0.05$), and the different characters (a, b) signify the statistical difference between treatments associated with one UV lamp type and one relative humidity ($p < 0.05$). Error bars signify \pm standard deviation.

4. Discussion

4.1. Ammonia and Hydrogen Sulfide

In this study, NH_3 mitigation was only effective when photocatalysis was used, regardless of the type of UV lamp, which is generally consistent with previous research. Research [37,38] suggests that a shorter wavelength (e.g., 220 nm) is needed to mitigate NH_3 with photolysis. Other researchers have also reported on the weak adsorption of NH_3 to the TiO_2 coated surface at room temperature [39,40].

The greatest mitigation of NH_3 was at 12% RH in photocatalysis. The % reduction decreased with either dry air or increasing RH. In general, the higher % reduction is achieved under low (or dry) humidity conditions. This is due to the adsorption of water on the TiO_2 surface [39,41,42], which, in turn, inhibits the mitigation of the target substances [43–45]. A similar trend (at least for low RH) was observed in this study. However, the % reduction was found to be decreased in the dry condition, which was expected to show the highest % reduction. One explanation could be that the decreased % reduction in dry conditions is due to the absence of HO radicals produced by the photocatalysis of water. HO radicals make it easier to oxidize NH_3 [46]. The optimal RH for the % reduction is different depending on the type of target gas. The comparison of optimum RH for selected target gases in the photocatalysis is summarized in Table 5.

Table 5. Comparison of optimum relative humidity for each target gases in the photocatalysis.

Reference	Target Gas	UV Type (Wavelength)	Coating Material (Dose)	The Relative Humidity Condition for Optimal % Reduction
[42]	Ammonia	UV-A (355 nm)	TiO_2 -P25 (650 $\mu\text{g}\cdot\text{cm}^{-2}$)	Low > High
[43]	Toluene	UV-A (315–400 nm)	TiO_2 -P25 (Not reported)	Dry (1%)
[44]	Acetaldehyde	UV-A (365 nm)	TiO_2 (Not reported)	Dry
[47]	Trichloroethylene	UV-A (Not reported)	TiO_2 sol-gel films (~1 $\text{mg}\cdot\text{cm}^{-2}$)	<50%
[48]	Trichloroethylene	UV-A (Not reported)	TiO_2 -GFC (4.8 $\text{g}\cdot\text{cm}^{-2}$)	<25%
[49]	Hydrogen sulfide Volatile organic compounds	UV-A (Not reported)	TiO_2 -ceramic filter (Not reported)	No impact (40–80%)
[50]	Hydrocarbons mixture	Not reported (280–650 nm)	TiO_2 -P25 (Thickness of 1–2 mm)	Dry
This study	Ammonia	UV-A (365 nm)	TiO_2 (10 $\mu\text{g}\cdot\text{cm}^{-2}$)	12%

Table 6 summarize previous research on the % reduction of selected target gases important in animal production systems via photocatalysis with UV-A. The % reduction of NH_3 was ~30%, but it required longer treatment (>6 min). In this study, the % reduction was ~9% on average (max: 18.7%, min: 2.56%) and 200 s. In general, the % reduction increases as the UV light intensity and treatment time of photocatalysis action increase [38,47,51]. This study also showed an increase in NH_3 % reduction with increasing light intensity and treatment time.

Table 6. Summary of mitigation for selected target gas in photocatalysis with UV-A.

Reference	Experiment Conditions	Coating Material	UV Type (Wavelength)	Light Intensity	Target Gas (% Ave ¹ Reduction)
[1]	Swine farm Temp ² : 21.8–26.0 °C RH ³ : 36–80% T time ⁴ (s): 24, 47	TiO ₂ (10 µg·cm ⁻²)	UV-A (365 nm)	<0.04 mW·cm ⁻²	CH ₄ (−2.2) CO ₂ (−3.1) N ₂ O (8.7) Odor (16.3) <i>p</i> -cresol (22.0)
[18]	Swine farm Temp: 25.7 °C RH: 56.0% CMM: 271.1 T time (s): 71.6	TiO ₂ (7 mg·cm ⁻²)	UV-A (315–400 nm)	Not reported	NH ₃ (2.0), CH ₄ (27.4) CO ₂ (−4.5) N ₂ O (−0.8) PM ₁₀ (17.0) PM _{2.5} (−8.1)
[19]	Swine farm Temp: 24.3 °C RH: 53.6% CMM: 74.9 T time (s): 364.2	TiO ₂ (7 mg·cm ⁻²)	UV-A (315–400 nm)	Not reported	NH ₃ (30.5), CH ₄ (10.8), CO ₂ (15.3) N ₂ O (4.2)
[52]	Lab-scale Temp: 24 °C RH: 50 % T time (min): >30	TiO ₂ (Not reported)	UV-A (365 nm)	0.46 mW·cm ⁻²	NH ₃ (35.0)
This study	Lab-scale Temp: 25 ± 3 °C RH: Dry, 12%, 40%, 60% T time (s): 40, 200	TiO ₂ (10 µg·cm ⁻²)	UV-A (365 nm)	0.44 vs. 4.85 mW·cm ⁻²	NH ₃ (4.8 vs. 9.3) H ₂ S (−2.1 vs. 1.7) CH ₄ (3.4 vs. 2.1) CO ₂ (−3.1 vs. 3.8) N ₂ O (3.3 vs. 6.6) O ₃ (22.6 vs. 34.7)

Note: ¹ Mean; ² Temperature; ³ Relative humidity; ⁴ Treatment time; Bold font signifies a statistical diff. ($p < 0.05$).

Photocatalysis was affected by dust accumulation. In particular, the increase in dust at high RH conditions canceled the NH₃ % reduction effect. This is because when dust accumulated, poultry dust continually increased the absorption of the UV light. Zhu et al. [21] reported that dust accumulation (in a swine barn) had no effect on the % reduction of VOCs. In this study, H₂S showed no % reduction effect in the treatment system using UV-A light and TiO₂ based photocatalysis. Previous studies with higher TiO₂ coating density and light intensity have shown a mitigation effect [53,54].

4.2. Greenhouse Gases and Ozone

CH₄ was not affected by any treatment in this study. The results add to a mixed body of knowledge. Our previous study with PureTi coating [1] did not show a statistically significant % reduction. Another research reported photocatalytic CH₄ % reduction at a low product yield and low energy efficiency [55]. However, two previous studies [18,19] (UV-A light) reported an 11–27% reduction. The reasons for our lack of apparent treatment could be due to low TiO₂ coating density, and the possibility that the mitigation effect was offset by forming CH₄ from the reduction of CO₂ [56–58].

CO₂ showed a 3.8% mitigation only under the RH of 12% with 200 s of LED irradiation. Although there is previous research demonstrating photocatalytic reduction of CO₂ to CH₄ under specific conditions [59], there is no chemical reason to expect that photocatalysis under these conditions (aerobic atmosphere and standard TiO₂ catalyst) could reduce CO₂; in fact, CO₂ is the oxidative endpoint for photocatalytic oxidation of virtually all carbon-containing compounds. It is thus tempting to suggest that an indirect mechanism for any observed CO₂ mitigation must exist, such as conversion to carbonates or surface absorption. By whatever mechanism, similar CO₂ concentration reductions were also observed by previous studies [19,58].

N₂O and O₃ were mitigated in both direct photolysis and photocatalysis. In general, N₂O and O₃ are known not to absorb significantly in the UV-A range, meaning that they are not subject to direct photolytic degradation at these wavelengths. However, indirect effects through more complex reaction paths can certainly affect their observed concentrations. Similarly, under photocatalytic conditions, where direct absorption by the substrate is not required, reasonably direct removal can occur. Previous research [60] reported that the N₂O photolysis rate was inhibited at >230 nm, and [61] reported that O₃ % reduction does not occur efficiently at >305 nm. However, this and our previous study [1] showed the mitigation effect of N₂O and O₃ under 365 nm. In the case of N₂O, the % reduction was about 3.3–6.5%, also in the case of O₃, the % reduction was 12.4–24.1% (Table 7).

Table 7. Comparison of mitigation of the N₂O and O₃ in photolysis and photocatalysis.

Reference	Treatment Time	Direct Photolysis	Photocatalysis
		Target Gas (% Reduction)	
[1]	24 s	N ₂ O (4.2)	N ₂ O (7.3)
	47 s	N ₂ O (7.6)	N ₂ O (8.7)
This study	40 s	N ₂ O (No % reduction)	N ₂ O (2.8–6.8)
		O ₃ (23.5)	O ₃ (21.6–37.0)
	200 s	N ₂ O (3.3–6.5)	N ₂ O (3.7–9.5)
		O ₃ (12.4–24.1)	O ₃ (21.8–48.4)

As expected, photocatalysis showed higher mitigation for N₂O than direct photolysis. However, this study result is quite different from those of previous studies. This is because previous research [20,37,38,51,52,62] indicates that by-products like N₂O and N₂ are generated via photocatalysis reaction in the presence of NH₃, but the levels of N₂O and N₂ vary according to treatment conditions and wavelength. Only one previous study showed a consistent trend with this study [1]. In theory, TiO₂ could only be activated by UV light with a wavelength of <387.5 nm due to its considerable bandgap energy [63,64]. Also, N₂O has been reported to be mitigated with UV-A, although its efficiency is lower than that of UV-C [63]. How much of this process actually decrease the N₂O produced by NH₃ decomposition has not been investigated in this study. However, the low but statistically significant % reduction could be due to other factors such as direct reduction by photocatalysis, indirect reduction by electrochemical reactions during the decomposition of other substances such as O₃, and adsorption of by-products on the TiO₂.

In the case of O₃, the previous results are different depending on the type of TiO₂ coating material, but it is reported that O₃ reduction does not occur >290 nm with TiO₂ [65]. However, O₃ has been reported to increase the reduction of target gas through the formation of ozonide radicals during photocatalysis [66–69]. Thus, during photocatalysis, O₃ concentration can be reduced due to the formation of ozonide radicals that are beneficial for reducing other target gases. In this study, the % reduction was 3.4–9.7% for N₂O and 20.4–48.4% for O₃.

5. Conclusions

The results of the study provide evidence that photocatalysis with TiO₂ coating and UV-A light can reduce gas concentrations of NH₃, CO₂, N₂O, and O₃, without significant effect on H₂S and CH₄. The particular % reduction depends on the presence of photocatalyst, RH, light type (intensity), treatment time, and dust accumulation on the photocatalyst surface. In the case of NH₃, the % reduction varied from 2.6–18.7% and was affected by RH and light intensity. The % reduction of NH₃ was the highest at 12% RH and increased with treatment time and light intensity. The % reduction of NH₃ decreased with the accumulation of poultry dust. The % reduction for H₂S had no statistical difference under any experimental conditions. The proposed treatment of NH₃ and H₂S was evaluated for a potential impact on important ambient air quality parameters, the possibility of simultaneously

mitigating/generating GHGs. There was no statistically significant change in CH₄ concentrations under any tested conditions. CO₂ was reduced at 3.8–4.4%. N₂O and O₃ concentrations were reduced by both direct photolysis and photocatalysis, with the latter having greater % reductions. As much as 6.9–12.2% of the statistically-significant % reduction of N₂O was observed. The % reduction for O₃ ranged from 12.4–48.4%. The results warrant scaling up to pilot-scale where the technology could be evaluated with economic analyses. It is necessary to investigate the practical applicability to the real system through large scale studies.

Author Contributions: Conceptualization, J.A.K., W.J.; methodology, J.A.K.; validation, M.L., J.W., H.A., & J.A.K.; formal analysis, M.L., J.W.; investigation, M.L., J.W., P.L., B.C., Z.M., & C.B.; resources, P.L., B.C., Z.M., C.B., and J.A.K.; data curation, M.L., J.A.K.; writing—original draft preparation, M.L.; writing—review and editing, M.L., H.A., J.A.K., & W.J.; visualization, M.L.; supervision, H.A., J.A.K.; project administration, J.A.K., W.J.; funding acquisition, J.A.K., W.J. All authors have read and agreed to the published version of the manuscript.

Funding: This research was supported by US Poultry & Egg Association Project #F080 “Mitigation of Ammonia and Odor Emissions: Improving Indoor Air Quality in Poultry Housing with Black UV Light.” The research was made possible in part by an endowing Foundation gift from Koch Foods. This research was partially supported by the Iowa Agriculture and Home Economics Experiment Station, Ames, Iowa. Project no. IOW05556 (Future Challenges in Animal Production Systems: Seeking Solutions through Focused Facilitation) sponsored by Hatch Act & State of Iowa funds. The authors would like to thank the Ministry of Education and Science of the Republic of Kazakhstan for supporting Zhanibek Meiirkhanuly with a Master of Science (M.S.) study scholarship via the Bolashak Program.

Acknowledgments: This authors gratefully acknowledge Woosang Lee (Smart Control & Sensing Inc.) for his help with the gas monitoring system, Cameron Hall (ISU Poultry Teaching Farm) for facilitating the on-farm collection of poultry dust, Aaron Stephan and Hoa-Thanh Huynh from ONCE Innovations for the LED array and Bikash Rajkarnikar (PureTi) for coating with a photocatalyst.

Conflicts of Interest: The author does not declare a conflict of interest. The funders did not play any role in the study design, data collection, analysis, interpretation, and decision to write a manuscript or present results.

Appendix A

Table A1. NH₃ mitigation under different light types and relative humidity at a treatment time of 40 s. Value in the table report % reduction ± standard deviation (*p*-value). Bold font signifies statistical significance.

Relative Humidity	Type of UV lamp	Direct Photolysis (UV only)	Photocatalysis (UV + TiO ₂)	Adsorption (to TiO ₂)
Dry	Fluorescent LED	0.0 ± 0.0	2.6 ± 0.8 (0.03)	1.2 ± 2.0
		1.2 ± 2.0	3.8 ± 1.3 (0.04)	2.7 ± 2.7
12%	Fluorescent LED	−1.2 ± 2.0	7.3 ± 0.6 (0.00)	2.0 ± 1.8
		0.0 ± 0.0	10.4 ± 3.4 (0.03)	4.3 ± 2.1
40%	Fluorescent LED	0.0 ± 0.0	5.0 ± 1.5 (0.03)	0.0 ± 0.0
		0.0 ± 0.0	7.3 ± 1.2 (0.00)	1.2 ± 2.0
60%	Fluorescent LED	0.0 ± 0.0	3.1 ± 0.4 (0.01)	1.1 ± 1.9
		0.0 ± 0.0	5.1 ± 3.1 (0.08)	2.1 ± 1.8
Average	Fluorescent LED	−0.3 ± 1.0	4.5 ± 2.1	1.1 ± 1.6
		0.3 ± 1.0	6.7 ± 3.3	2.6 ± 2.2

Table A2. NH₃ mitigation under different light types and relative humidity at a treatment time of 200 s. Values in the table report % reduction \pm standard deviation (*p*-value). Bold font signifies statistical significance.

Relative Humidity	Type of UV Lamp	Direct Photolysis (UV only)	Photocatalysis (UV + TiO ₂)	Adsorption (to TiO ₂)
Dry	Fluorescent LED	0.0 \pm 0.0	3.1 \pm 0.4 (0.00)	2.2 \pm 1.9
		0.0 \pm 0.0	5.2 \pm 1.6 (0.03)	3.0 \pm 2.8
12%	Fluorescent LED	0.0 \pm 0.0	9.4 \pm 1.3 (0.00)	4.0 \pm 3.5
		0.0 \pm 0.0	18.7 \pm 2.0 (0.00)	1.8 \pm 1.6
40%	Fluorescent LED	0.0 \pm 0.0	5.3 \pm 2.4 (0.05)	1.1 \pm 1.9
		0.0 \pm 0.0	13.5 \pm 2.6 (0.01)	2.0 \pm 1.8
60%	Fluorescent LED	0.0 \pm 0.0	3.2 \pm 0.4 (0.00)	0.0 \pm 0.0
		1.9 \pm 3.2	6.2 \pm 0.6 (0.00)	1.9 \pm 3.2
Average	Fluorescent LED	0.0 \pm 0.0	5.3 \pm 2.9	1.8 \pm 2.4
		0.5 \pm 1.6	10.9 \pm 6.0	2.2 \pm 2.1

Table A3. NH₃ mitigation under the different dust levels at a relative humidity of dry and 12%. Values in the table report % reduction \pm standard deviation (*p*-value). Bold font signifies statistical significance.

Relative Humidity		Dry		12%	
Treatment Time		40 s	200 s	40 s	200 s
No dust	Fluorescent LED	2.6 \pm 0.8 (0.03)	3.1 \pm 0.4 (0.00)	7.3 \pm 0.6 (0.00)	9.4 \pm 1.3 (0.00)
		3.8 \pm 1.3 (0.04)	5.2 \pm 1.6 (0.03)	10.4 \pm 3.4 (0.03)	18.7 \pm 2.0 (0.00)
Dust (6.9 mg·cm ⁻²)	Fluorescent LED	3.1 \pm 0.5 (0.00)	4.2 \pm 2.2 (0.07)	6.2 \pm 0.8 (0.00)	9.2 \pm 2.0 (0.01)
		4.0 \pm 1.0 (0.02)	5.0 \pm 1.8 (0.03)	11.1 \pm 1.9 (0.01)	16.2 \pm 3.2 (0.01)
Dust (11.0 mg·cm ⁻²)	Fluorescent LED	1.1 \pm 1.9 (0.42)	3.3 \pm 5.8 (0.43)	5.1 \pm 1.7 (0.03)	7.2 \pm 0.8 (0.00)
		4.2 \pm 2.0 (0.07)	3.1 \pm 0.4 (0.00)	8.1 \pm 1.5 (0.01)	9.2 \pm 0.9 (0.00)
Dust (16.3 mg·cm ⁻²)	Fluorescent LED	0.9 \pm 1.5 (0.42)	2.0 \pm 1.7 (0.19)	0.9 \pm 1.6 (0.42)	4.0 \pm 3.5 (0.18)
		2.0 \pm 1.7 (0.17)	2.8 \pm 2.6 (0.20)	5.1 \pm 1.7 (0.03)	6.7 \pm 3.4 (0.08)

Table A4. NH₃ mitigation under the different dust levels at a relative humidity of 40% and 60%. Value in the table report % reduction \pm standard deviation (*p*-value).

Relative Humidity		40%		60%	
Treatment Time		40 s	200 s	40 s	200 s
No dust	Fluorescent LED	5.0 \pm 1.5 (0.03)	5.3 \pm 2.4 (0.05)	3.1 \pm 0.4 (0.01)	3.2 \pm 0.4 (0.00)
		7.3 \pm 1.2 (0.00)	13.5 \pm 2.6 (0.01)	5.1 \pm 3.1 (0.08)	6.2 \pm 0.6 (0.00)
Dust (6.9 mg·cm ⁻²)	Fluorescent LED	3.1 \pm 3.4 (0.25)	4.3 \pm 2.1 (0.08)	2.0 \pm 1.7 (0.18)	2.9 \pm 2.7 (0.20)
		8.4 \pm 4.3 (0.07)	10.5 \pm 2.7 (0.02)	5.1 \pm 1.7 (0.03)	6.8 \pm 3.6 (0.08)
Dust (11.0 mg·cm ⁻²)	Fluorescent LED	2.0 \pm 1.8 (0.19)	2.9 \pm 2.7 (0.21)	3.2 \pm 3.2 (0.23)	1.8 \pm 3.1 (0.82)
		6.2 \pm 3.4 (0.08)	5.1 \pm 1.7 (0.03)	4.0 \pm 1.1 (0.02)	6.2 \pm 0.6 (0.00)
Dust (16.3 mg·cm ⁻²)	Fluorescent LED	0.0 \pm 0.0 (1.00)	1.1 \pm 1.9 (0.42)	0.0 \pm 0.0 (1.00)	0.0 \pm 0.0 (1.00)
		2.3 \pm 4.0 (0.47)	5.3 \pm 2.4 (0.05)	4.3 \pm 4.9 (0.27)	4.0 \pm 1.3 (0.03)

Table A5. CO₂ mitigation under the different dust levels at a relative humidity of 12%. Values in the table report % reduction \pm standard deviation (*p*-value) and are an average between treatments of NH₃ and H₂S standard gases. Bold font signifies statistical significance.

Dust level	Type of UV Lamp	Photocatalysis at A Treatment Time of 40 s (UV + TiO ₂)	Photocatalysis at A Treatment Time of 200 s (UV + TiO ₂)
No dust	Fluorescent LED	1.4 \pm 3.4 (0.57) 4.2 \pm 3.3 (0.17)	6.5 \pm 6.2 (0.23) 3.8 \pm 0.7 (0.01)
Dust (6.9 mg·cm ⁻²)	Fluorescent LED	1.5 \pm 4.1 (0.56) −0.7 \pm 6.6 (0.96)	0.9 \pm 15.2 (0.90) 3.5 \pm 7.7 (0.50)
Dust (11.0 mg·cm ⁻²)	Fluorescent LED	3.5 \pm 7.7 (0.50) 0.5 \pm 4.4 (0.91)	2.7 \pm 7.7 (0.55) −1.3 \pm 3.3 (0.54)
Dust (16.3 mg·cm ⁻²)	Fluorescent LED	4.2 \pm 3.5 (0.17) 0.4 \pm 8.8 (0.65)	−2.5 \pm 7.1 (0.59) 0.7 \pm 5.6 (0.90)

Table A6. N₂O mitigation under different light types and relative humidity at a treatment time of 40 s. Values in the table report % reduction \pm standard deviation (*p*-value) and are an average between treatments of NH₃ and H₂S standard gases. Bold font signifies statistical significance.

Relative Humidity	Type of UV Lamp	Direct Photolysis (UV only)	Photocatalysis (UV + TiO ₂)	Adsorption (to TiO ₂)
Dry	Fluorescent LED	1.6 \pm 2.0 2.7 \pm 1.2	4.8 \pm 4.9 (0.14) 6.5 \pm 2.5 (0.02)	3.0 \pm 1.5 −0.6 \pm 3.5
12%	Fluorescent LED	2.1 \pm 2.1 3.3 \pm 1.8	3.1 \pm 2.9 (0.06) 9.0 \pm 5.2 (0.05)	1.8 \pm 3.5 3.2 \pm 10.9
40%	Fluorescent LED	1.8 \pm 0.8 3.1 \pm 2.1	3.4 \pm 0.2 (0.00) 6.8 \pm 1.7 (0.01)	1.6 \pm 3.2 −1.4 \pm 2.1
60%	Fluorescent LED	2.5 \pm 3.3 3.7 \pm 2.4	2.8 \pm 0.7 (0.03) 5.2 \pm 3.3 (0.07)	−1.0 \pm 3.5 2.2 \pm 2.7
Average	Fluorescent LED	2.0 \pm 1.9 3.2 \pm 1.7	3.5 \pm 2.7 6.7 \pm 3.4	1.8 \pm 2.9 0.9 \pm 5.5

Table A7. N₂O mitigation under different light types and relative humidity at a treatment time of 200 s. Values in the table report % reduction \pm standard deviation (*p*-value) and are an average between treatments of NH₃ and H₂S standard gases. Bold font signifies statistical significance.

Relative Humidity	Type of UV Lamp	Direct Photolysis (UV only)	Photocatalysis (UV + TiO ₂)	Adsorption (to TiO ₂)
Dry	Fluorescent LED	1.3 \pm 1.5 3.3 \pm 1.2 (0.04)	3.7 \pm 1.8 (0.03) 5.1 \pm 1.0 (0.00)	2.5 \pm 2.8 4.4 \pm 2.8
12%	Fluorescent LED	1.8 \pm 1.6 6.5 \pm 1.7 (0.02)	3.3 \pm 2.1 (0.07) 9.5 \pm 3.3 (0.02)	1.4 \pm 1.7 0.8 \pm 5.2
40%	Fluorescent LED	1.3 \pm 1.1 4.9 \pm 4.4	3.0 \pm 2.3 (0.06) 10.6 \pm 6.6 (0.06)	0.2 \pm 0.4 3.1 \pm 4.0
60%	Fluorescent LED	1.0 \pm 0.8 0.8 \pm 0.5	5.6 \pm 3.8 (0.08) 5.0 \pm 0.9 (0.00)	−2.1 \pm 3.5 2.2 \pm 1.4
Average	Fluorescent LED	1.7 \pm 1.2 3.9 \pm 3.0	3.9 \pm 2.5 7.5 \pm 4.3	0.5 \pm 2.7 2.6 \pm 3.4

Table A8. N₂O mitigation under the different dust levels at a treatment time of 200 s in direct photolysis. Values in the table report % reduction \pm standard deviation (*p*-value) and are an average between treatments of NH₃ and H₂S standard gases. Bold font signifies statistical significance.

Relative Humidity		Dry	12%	40%	60%
No Dust	Fluorescent	1.3 \pm 1.5 (0.32)	1.8 \pm 1.6 (0.20)	1.3 \pm 1.1 (0.15)	1.0 \pm 0.8 (0.16)
	LED	3.3 \pm 1.2 (0.04)	6.5 \pm 1.7 (0.02)	4.9 \pm 4.4 (0.15)	0.8 \pm 0.5 (0.12)
Dust (6.9 mg·cm ⁻²)	Fluorescent	1.0 \pm 0.5 (0.08)	4.1 \pm 6.9 (0.41)	4.4 \pm 4.3 (0.23)	3.5 \pm 6.0 (0.41)
	LED	1.6 \pm 0.4 (0.03)	6.1 \pm 3.0 (0.08)	5.3 \pm 1.7 (0.03)	5.2 \pm 3.3 (0.13)
Dust (11.0 mg·cm ⁻²)	Fluorescent	1.1 \pm 1.8 (0.40)	4.2 \pm 3.0 (0.08)	5.0 \pm 9.6 (0.45)	3.2 \pm 1.1 (0.03)
	LED	2.8 \pm 1.4 (0.06)	4.0 \pm 1.7 (0.06)	4.8 \pm 2.5 (0.05)	5.9 \pm 5.0 (0.18)
Dust (16.3 mg·cm ⁻²)	Fluorescent	2.5 \pm 2.1 (0.18)	2.4 \pm 2.1 (0.22)	7.2 \pm 6.3 (0.19)	4.8 \pm 3.6 (0.10)
	LED	1.4 \pm 0.8 (0.10)	4.2 \pm 7.0 (0.40)	5.0 \pm 9.5 (0.45)	7.1 \pm 6.3 (0.19)

Table A9. N₂O mitigation under the different dust levels at a relative humidity of dry and 12% in photocatalysis. Values in the table report % reduction \pm standard deviation (*p*-value) and are an average between treatments of NH₃ and H₂S standard gases. Bold font signifies statistical significance.

Relative Humidity		Dry		12%	
Treatment Time		40 s	200 s	40 s	200 s
No Dust	Fluorescent	4.8 \pm 4.9 (0.14)	3.7 \pm 1.8 (0.03)	3.1 \pm 2.9 (0.06)	3.3 \pm 2.1 (0.07)
	LED	6.5 \pm 2.5 (0.02)	5.1 \pm 1.0 (0.00)	9.0 \pm 5.2 (0.05)	9.5 \pm 3.3 (0.02)
Dust (6.9 mg·cm ⁻²)	Fluorescent	8.5 \pm 4.3 (0.09)	3.1 \pm 2.2 (0.14)	10.5 \pm 3.9 (0.06)	3.2 \pm 0.9 (0.03)
	LED	4.7 \pm 5.9 (0.30)	4.2 \pm 2.0 (0.04)	5.1 \pm 3.4 (0.12)	11.2 \pm 2.1 (0.04)
Dust (11.0 mg·cm ⁻²)	Fluorescent	4.1 \pm 3.1 (0.16)	5.3 \pm 2.2 (0.05)	4.1 \pm 3.7 (0.20)	1.0 \pm 2.3 (0.53)
	LED	5.0 \pm 1.6 (0.04)	4.2 \pm 3.3 (0.16)	3.7 \pm 3.2 (0.18)	4.2 \pm 3.7 (0.20)
Dust (16.3 mg·cm ⁻²)	Fluorescent	3.6 \pm 5.5 (0.35)	5.3 \pm 3.9 (0.14)	8.9 \pm 6.2 (0.14)	3.3 \pm 6.9 (0.41)
	LED	5.7 \pm 5.6 (0.23)	2.8 \pm 0.5 (0.00)	3.4 \pm 0.3 (0.01)	4.7 \pm 2.0 (0.04)

Table A10. N₂O mitigation under the different dust levels at a relative humidity of 40% and 60% in photocatalysis. Values in the table report % reduction \pm standard deviation (*p*-value) and are an average between treatments of NH₃ and H₂S standard gases. Bold font signifies statistical significance.

Relative Humidity		40%		60%	
Treatment Time		40 s	200 s	40 s	200 s
No Dust	Fluorescent	3.4 \pm 0.2 (0.00)	3.0 \pm 2.3 (0.06)	2.8 \pm 0.7 (0.03)	5.6 \pm 3.8 (0.08)
	LED	6.8 \pm 1.7 (0.01)	10.6 \pm 6.6 (0.06)	5.2 \pm 3.3 (0.07)	5.0 \pm 0.9 (0.00)
Dust (6.9 mg·cm ⁻²)	Fluorescent	4.6 \pm 2.0 (0.07)	6.2 \pm 1.8 (0.04)	2.4 \pm 6.2 (0.54)	2.1 \pm 6.2 (0.67)
	LED	5.3 \pm 2.1 (0.05)	7.9 \pm 2.3 (0.01)	4.5 \pm 2.3 (0.09)	7.1 \pm 6.4 (0.20)
Dust (11.0 mg·cm ⁻²)	Fluorescent	11.3 \pm 7.2 (0.13)	1.0 \pm 2.3 (0.52)	3.3 \pm 3.1 (0.20)	5.6 \pm 2.4 (0.05)
	LED	2.8 \pm 3.0 (0.22)	5.3 \pm 3.9 (0.14)	3.6 \pm 5.5 (0.37)	3.7 \pm 6.3 (0.41)
Dust (16.3 mg·cm ⁻²)	Fluorescent	7.4 \pm 6.2 (0.20)	3.9 \pm 5.9 (0.36)	5.1 \pm 3.3 (0.12)	6.8 \pm 6.8 (0.18)
	LED	2.4 \pm 3.2 (0.32)	1.0 \pm 2.2 (0.52)	1.4 \pm 1.3 (0.19)	3.8 \pm 5.8 (0.36)

Table A11. O₃ mitigation under different light types and relative humidity at a treatment time of 40 s. Values in the table report % reduction \pm standard deviation (*p*-value) and are an average between treatments of NH₃ and H₂S standard gases. Bold font signifies statistical significance.

Relative Humidity	Type of UV Lamp	Direct Photolysis (UV only)	Photocatalysis (UV + TiO ₂)	Adsorption (to TiO ₂)
Dry	Fluorescent LED	14.9 \pm 5.4 (0.05) 16.1 \pm 12.1 (0.16)	22.3 \pm 16.2 (0.07) 29.7 \pm 2.6 (0.00)	5.3 \pm 9.1 2.7 \pm 21.6
12%	Fluorescent LED	11.8 \pm 10.7 (0.19) 26.0 \pm 11.6 (0.08)	21.2 \pm 13.5 (0.06) 37.0 \pm 6.9 (0.03)	5.1 \pm 5.6 −1.1 \pm 1.9
40%	Fluorescent LED	14.9 \pm 10.6 (0.11) 23.5 \pm 4.2 (0.00)	27.4 \pm 17.1 (0.15) 36.0 \pm 7.1 (0.02)	4.2 \pm 7.2 1.8 \pm 16.1
60%	Fluorescent LED	11.3 \pm 4.9 (0.06) 31.5 \pm 14.1 (0.07)	21.6 \pm 2.4 (0.00) 27.6 \pm 16.0 (0.17)	8.9 \pm 7.7 4.2 \pm 7.2
Average	Fluorescent LED	13.2 \pm 7.3 24.3 \pm 11.1	23.1 \pm 12.5 32.6 \pm 9.4	5.9 \pm 6.7 1.9 \pm 12.1

Table A12. O₃ mitigation under different light types and relative humidity at 200 s. Values report % reduction \pm st. dev. (*p*-value) and are an average between treatments of NH₃ and H₂S. Bold font signifies statistical significance.

Relative Humidity	Type of UV Lamp	Direct Photolysis (UV only)	Photocatalysis (UV + TiO ₂)	Adsorption (to TiO ₂)
Dry	Fluorescent LED	13.3 \pm 5.2 (0.05) 12.8 \pm 3.1 (0.01)	22.5 \pm 5.4 (0.04) 28.7 \pm 3.7 (0.00)	6.0 \pm 7.4 3.0 \pm 2.6
12%	Fluorescent LED	12.4 \pm 3.8 (0.03) 12.9 \pm 0.8 (0.00)	23.7 \pm 2.6 (0.00) 48.4 \pm 5.3 (0.00)	2.5 \pm 5.6 5.4 \pm 6.1
40%	Fluorescent LED	10.8 \pm 6.1 (0.09) 8.9 \pm 4.7 (0.09)	21.8 \pm 5.3 (0.00) 26.0 \pm 5.2 (0.01)	7.0 \pm 9.1 5.0 \pm 1.6
60%	Fluorescent LED	18.2 \pm 10.4 (0.11) 24.1 \pm 7.9 (0.03)	23.6 \pm 0.7 (0.00) 37.5 \pm 5.1 (0.00)	6.1 \pm 3.5 1.8 \pm 5.9
Average	Fluorescent LED	13.7 \pm 6.5 14.7 \pm 7.3	22.9 \pm 3.7 35.2 \pm 10.0	5.4 \pm 6.0 3.3 \pm 4.1

Table A13. O₃ mitigation under the different dust levels at a relative humidity of dry and 12% in direct photolysis. Value in the table report % reduction \pm standard deviation (*p*-value) and are an average between treatments of NH₃ and H₂S standard gases. Bold font signifies statistical significance.

Relative Humidity		Dry		12%	
Treatment Time		40 s	200 s	40 s	200 s
No dust	Fluorescent LED	14.9 \pm 5.4 (0.05)	13.3 \pm 5.2 (0.05)	11.8 \pm 10.7 (0.19)	12.4 \pm 3.8 (0.03)
		16.1 \pm 12.1 (0.16)	12.8 \pm 3.1 (0.01)	26.0 \pm 11.6 (0.08)	12.9 \pm 0.8 (0.00)
Dust (6.9 mg·cm ^{−2})	Fluorescent LED	11.4 \pm 5.2 (0.05)	21.0 \pm 12.8 (0.10)	12.1 \pm 8.5 (0.15)	13.1 \pm 5.7 (0.06)
		14.7 \pm 9.5 (0.12)	19.8 \pm 8.9 (0.07)	38.0 \pm 16.9 (0.05)	15.6 \pm 8.5 (0.09)
Dust (11.0 mg·cm ^{−2})	Fluorescent LED	14.4 \pm 1.4 (0.00)	19.0 \pm 11.6 (0.11)	16.7 \pm 8.5 (0.08)	18.4 \pm 5.9 (0.03)
		22.5 \pm 12.3 (0.09)	16.0 \pm 0.8 (0.00)	25.5 \pm 11.5 (0.06)	26.3 \pm 10.4 (0.05)
Dust (16.3 mg·cm ^{−2})	Fluorescent LED	16.1 \pm 11.1 (0.12)	21.2 \pm 10.5 (0.09)	17.8 \pm 8.8 (0.08)	11.6 \pm 6.6 (0.09)
		15.6 \pm 10.1 (0.12)	29.4 \pm 22.0 (0.19)	21.8 \pm 6.6 (0.03)	25.8 \pm 8.4 (0.04)

Table A14. O₃ mitigation under the different dust levels at a relative humidity of 40% and 60% in photolysis. Value in the table report % reduction \pm standard deviation (*p*-value) and are an average between treatments of NH₃ and H₂S standard gases. Bold font signifies statistical significance.

Relative Humidity		40%		60%	
Treatment Time		40 s	200 s	40 s	200 s
No Dust	Fluorescent	14.9 \pm 10.6 (0.11)	10.8 \pm 6.1 (0.09)	11.3 \pm 4.9 (0.06)	18.2 \pm 10.4 (0.11)
	LED	23.5 \pm 4.2 (0.00)	8.9 \pm 4.7 (0.09)	31.5 \pm 14.1 (0.07)	24.1 \pm 7.9 (0.03)
Dust (6.9 mg·cm ⁻²)	Fluorescent	20.6 \pm 9.7 (0.06)	13.8 \pm 3.3 (0.02)	29.0 \pm 4.7 (0.02)	13.6 \pm 7.1 (0.09)
	LED	19.1 \pm 3.7 (0.00)	15.4 \pm 2.2 (0.00)	18.3 \pm 2.5 (0.00)	17.9 \pm 9.5 (0.09)
Dust (11.0 mg·cm ⁻²)	Fluorescent	10.7 \pm 10.0 (0.20)	14.2 \pm 8.7 (0.11)	18.0 \pm 9.1 (0.08)	20.6 \pm 11.0 (0.10)
	LED	18.1 \pm 6.4 (0.06)	21.9 \pm 3.2 (0.00)	14.9 \pm 8.0 (0.09)	22.1 \pm 6.6 (0.03)
Dust (16.3 mg·cm ⁻²)	Fluorescent	16.2 \pm 6.0 (0.03)	20.8 \pm 19.6 (0.21)	17.5 \pm 18.9 (0.27)	21.4 \pm 13.3 (0.14)
	LED	18.1 \pm 7.4 (0.05)	13.5 \pm 4.74 (0.03)	18.9 \pm 5.7 (0.03)	18.0 \pm 3.4 (0.02)

Table A15. O₃ mitigation under the different dust levels at a relative humidity of dry and 12% in photocatalysis. Value in the table report % reduction \pm standard deviation (*p*-value) and are an average between treatments of NH₃ and H₂S standard gases. Bold font signifies statistical significance.

Relative Humidity		Dry		12%	
Treatment Time		40 s	200 s	40 s	200 s
No dust	Fluorescent	22.3 \pm 16.2 (0.07)	22.5 \pm 5.4 (0.04)	21.2 \pm 13.5 (0.06)	23.7 \pm 2.6 (0.00)
	LED	29.7 \pm 2.6 (0.00)	28.7 \pm 3.7 (0.00)	37.0 \pm 6.9 (0.03)	48.4 \pm 5.3 (0.00)
Dust (6.9 mg·cm ⁻²)	Fluorescent	18.4 \pm 3.0 (0.01)	32.8 \pm 5.6 (0.01)	26.7 \pm 9.6 (0.05)	36.9 \pm 2.8 (0.00)
	LED	21.7 \pm 9.5 (0.06)	38.1 \pm 7.8 (0.02)	35.3 \pm 7.2 (0.01)	29.0 \pm 1.6 (0.00)
Dust (11.0 mg·cm ⁻²)	Fluorescent	27.6 \pm 13.9(0.08)	33.1 \pm 6.3 (0.01)	33.7 \pm 11.1 (0.03)	34.0 \pm 10.0 (0.03)
	LED	28.4 \pm 8.0 (0.03)	40.5 \pm 3.7 (0.00)	44.9 \pm 1.8 (0.00)	44.1 \pm 11.5 (0.03)
Dust (16.3 mg·cm ⁻²)	Fluorescent	27.5 \pm 8.8 (0.03)	36.6 \pm 7.1 (0.02)	26.5 \pm 2.9 (0.00)	37.7 \pm 6.6 (0.01)
	LED	33.1 \pm 11.8(0.04)	48.9 \pm 13.9 (0.03)	33.9 \pm 10.0 (0.03)	48.9 \pm 4.1 (0.00)

Table A16. O₃ mitigation under the different dust levels at a relative humidity of 40% and 60% in photocatalysis. Value in the table report % reduction \pm standard deviation (*p*-value) and are an average between treatments of NH₃ and H₂S standard gases. Bold font signifies statistical significance.

Relative Humidity		40%		60%	
Treatment Time		40 s	200 s	40 s	200 s
No dust	Fluorescent	27.4 \pm 17.1 (0.15)	21.8 \pm 5.3 (0.00)	21.6 \pm 2.4 (0.00)	23.6 \pm 0.7 (0.00)
	LED	36.0 \pm 7.06 (0.02)	26.0 \pm 5.2 (0.01)	27.6 \pm 16.0 (0.17)	37.5 \pm 5.1 (0.00)
Dust (6.9 mg·cm ⁻²)	Fluorescent	20.9 \pm 5.3 (0.01)	23.4 \pm 0.8 (0.00)	35.5 \pm 10.4 (0.04)	22.8 \pm 2.8 (0.00)
	LED	30.7 \pm 12.4 (0.05)	25.3 \pm 1.7 (0.00)	32.2 \pm 2.6 (0.00)	29.4 \pm 9.8 (0.04)
Dust (11.0 mg·cm ⁻²)	Fluorescent	21.7 \pm 10.9 (0.08)	25.2 \pm 8.1 (0.04)	31.1 \pm 10.2 (0.03)	34.3 \pm 11.0 (0.04)
	LED	38.0 \pm 12.5 (0.05)	31.5 \pm 14.9 (0.06)	21.7 \pm 4.7 (0.02)	32.1 \pm 2.5 (0.00)
Dust (16.3 mg·cm ⁻²)	Fluorescent	22.6 \pm 5.6 (0.01)	30.0 \pm 9.9 (0.03)	34.4 \pm 10.0 (0.02)	34.5 \pm 9.6 (0.02)
	LED	36.5 \pm 6.6 (0.01)	38.9 \pm 10.0 (0.01)	42.8 \pm 10.2 (0.01)	34.9 \pm 4.3 (0.00)

References

1. Maurer, D.L.; Koziel, J.A. On-farm pilot-scale testing of black ultraviolet light and photocatalytic coating for mitigation of odor, odorous VOCs, and greenhouse gases. *Chemosphere* **2019**, *221*, 778–784. [[CrossRef](#)] [[PubMed](#)]
2. Buijsman, E.; Erisman, J.-W. Wet deposition of ammonium in Europe. *J. Atmos. Chem.* **1988**, *6*, 265–280. [[CrossRef](#)]
3. Schiffman, S.S. Livestock odors: Implications for human health and well-being. *J. Anim. Sci.* **1998**, *76*, 1343–1355. [[CrossRef](#)]
4. Maurer, D.L.; Koziel, J.A.; Harmon, J.D.; Hoff, S.J.; Rieck-Hinz, A.M.; Andersen, D.S. Summary of performance data for technologies to control gaseous, odor, and particulate emissions from livestock operations: Air management practices assessment tool (AMPAT). *Data Brief* **2016**, *7*, 1413–1429. [[CrossRef](#)]

5. Van der Heyden, C.; Demeyer, P.; Volcke, E.I. Mitigating emissions from pig and poultry housing facilities through air scrubbers and biofilters: State-of-the-art and perspectives. *Biosyst. Eng.* **2015**, *134*, 74–93. [[CrossRef](#)]
6. Maurer, D.; Koziel, J.; Kalus, K.; Andersen, D.; Opalinski, S. Pilot-scale testing of non-activated biochar for swine manure treatment and mitigation of ammonia, hydrogen sulfide, odorous volatile organic compounds (VOCs), and greenhouse gas emissions. *Sustainability* **2017**, *9*, 929. [[CrossRef](#)]
7. Maurer, D.L.; Koziel, J.A.; Bruning, K.; Parker, D.B. Farm-scale testing of soybean peroxidase and calcium peroxide for surficial swine manure treatment and mitigation of odorous VOCs, ammonia and hydrogen sulfide emissions. *Atmos. Environ.* **2017**, *166*, 467–478. [[CrossRef](#)]
8. Maurer, D.L.; Koziel, J.A.; Bruning, K.; Parker, D.B. Pilot-scale testing of renewable biocatalyst for swine manure treatment and mitigation of odorous VOCs, ammonia and hydrogen sulfide emissions. *Atmos. Environ.* **2017**, *150*, 313–321. [[CrossRef](#)]
9. Parker, D.B.; Hayes, M.; Brown-Brandl, T.; Woodbury, B.; Spiehs, M.; Koziel, J.A. Surface application of soybean peroxidase and calcium peroxide for reducing odorous VOC emissions from swine manure slurry. *Appl. Eng. Agric.* **2016**, *32*, 389–398. [[CrossRef](#)]
10. Cai, L.; Koziel, J.A.; Liang, Y.; Nguyen, A.T.; Xin, H. Evaluation of zeolite for control of odorants emissions from simulated poultry manure storage. *J. Environ. Qual.* **2007**, *36*, 184–193. [[CrossRef](#)]
11. Kalus, K.; Opaliński, S.; Maurer, D.; Rice, S.; Koziel, J.A.; Korczyński, M.; Dobrzański, Z.; Kołacz, R.; Gutarowska, B. Odour reducing microbial-mineral additive for poultry manure treatment. *Front. Environ. Sci. Eng.* **2017**, *11*, 7. [[CrossRef](#)]
12. Parker, D.B.; Pandrangi, S.; Greene, L.; Almas, L.; Cole, N.; Rhoades, M.; Koziel, J. Rate and frequency of urease inhibitor application for minimizing ammonia emissions from beef cattle feedyards. *Trans. ASAE* **2005**, *48*, 787–793. [[CrossRef](#)]
13. Parker, D.B.; Rhoades, M.B.; Koziel, J.A.; Baek, B.-H.; Waldrip, H.M.; Todd, R.W. Urease inhibitor for reducing ammonia emissions from an open-lot beef cattle feedyard in the Texas High Plains. *Appl. Eng. Agric.* **2016**, *32*, 823–832. [[CrossRef](#)]
14. Kalus, K.; Koziel, J.A.; Opaliński, S. A Review of Biochar Properties and Their Utilization in Crop Agriculture and Livestock Production. *Appl. Sci.* **2019**, *9*, 3494. [[CrossRef](#)]
15. Wi, J.; Lee, S.; Kim, E.; Lee, M.; Koziel, J.A.; Ahn, H. Evaluation of Semi-Continuous Pit Manure Recharge System Performance on Mitigation of Ammonia and Hydrogen Sulfide Emissions from a Swine Finishing Barn. *Atmosphere* **2019**, *10*, 170. [[CrossRef](#)]
16. Chen, L.; Hoff, S.; Cai, L.; Koziel, J.; Zelle, B. Evaluation of wood chip-based biofilters to reduce odor, hydrogen sulfide, and ammonia from swine barn ventilation air. *J. Air Waste Manag. Assoc.* **2009**, *59*, 520–530. [[CrossRef](#)] [[PubMed](#)]
17. Chen, L.; Hoff, S.J.; Koziel, J.A.; Cai, L.; Zelle, B.; Sun, G. Performance evaluation of a wood-chip based biofilter using solid-phase microextraction and gas chromatography–mass spectroscopy–olfactometry. *Bioresour. Technol.* **2008**, *99*, 7767–7780. [[CrossRef](#)] [[PubMed](#)]
18. Costa, A.; Chiarello, G.L.; Selli, E.; Guarino, M. Effects of TiO₂ based photocatalytic paint on concentrations and emissions of pollutants and on animal performance in a swine weaning unit. *J. Environ. Manag.* **2012**, *96*, 86–90. [[CrossRef](#)] [[PubMed](#)]
19. Guarino, M.; Costa, A.; Porro, M. Photocatalytic TiO₂ coating—To reduce ammonia and greenhouse gases concentration and emission from animal husbandries. *Bioresour. Technol.* **2008**, *99*, 2650–2658. [[CrossRef](#)]
20. Rockafellow, E.M.; Koziel, J.A.; Jenks, W.S. Laboratory-scale investigation of UV treatment of ammonia for livestock and poultry barn exhaust applications. *J. Environ. Qual.* **2012**, *41*, 281–288. [[CrossRef](#)]
21. Zhu, W.; Koziel, J.; Maurer, D. Mitigation of livestock odors using black light and a new titanium dioxide-based catalyst: Proof-of-concept. *Atmosphere* **2017**, *8*, 103. [[CrossRef](#)]
22. Hashimoto, K.; Irie, H.; Fujishima, A. TiO₂ photocatalysis: A historical overview and future prospects. *Jpn. J. Appl. Phys.* **2005**, *44*, 8269. [[CrossRef](#)]
23. Schneider, J.; Matsuoka, M.; Takeuchi, M.; Zhang, J.; Horiuchi, Y.; Anpo, M.; Bahnemann, D.W. Understanding TiO₂ photocatalysis: Mechanisms and materials. *Chem. Rev.* **2014**, *114*, 9919–9986. [[CrossRef](#)]
24. Zaleska, A. Doped-TiO₂: A review. *Recent Pat. Eng.* **2008**, *2*, 157–164. [[CrossRef](#)]
25. Lee, H.J.; Park, Y.G.; Lee, S.H.; Park, J.H. Photocatalytic Properties of TiO₂ According to Manufacturing Method. *Korean Chem. Eng. Res.* **2018**, *56*, 156–161. [[CrossRef](#)]

26. Vautier, M.; Guillard, C.; Herrmann, J.-M. Photocatalytic degradation of dyes in water: Case study of indigo and of indigo carmine. *J. Catal.* **2001**, *201*, 46–59. [\[CrossRef\]](#)
27. Jia, J.; Li, D.; Wan, J.; Yu, X. Characterization and mechanism analysis of graphite/C-doped TiO₂ composite for enhanced photocatalytic performance. *J. Ind. Eng. Chem.* **2016**, *33*, 162–169. [\[CrossRef\]](#)
28. Abe, R. Recent progress on photocatalytic and photoelectrochemical water splitting under visible light irradiation. *J. Photochem. Photobiol. C Photochem. Rev.* **2010**, *11*, 179–209. [\[CrossRef\]](#)
29. Maeda, K.; Domen, K. Photocatalytic water splitting: Recent progress and future challenges. *J. Phys. Chem. Lett.* **2010**, *1*, 2655–2661. [\[CrossRef\]](#)
30. Yang, X.; Zhu, W.; Koziel, J.A.; Cai, L.; Jenks, W.S.; Laor, Y.; van Leeuwen, J.H.; Hoff, S.J. Improved quantification of livestock associated odorous volatile organic compounds in a standard flow-through system using solid-phase microextraction and gas chromatography–mass spectrometry. *J. Chromatogr. A* **2015**, *1414*, 31–40. [\[CrossRef\]](#)
31. Valentine, H. A study of the effect of different ventilation rates on the ammonia concentrations in the atmosphere of broiler houses. *Br. Poult. Sci.* **1964**, *5*, 149–159. [\[CrossRef\]](#)
32. Wathes, C.; Holden, M.; Sneath, R.; White, R.; Phillips, V. Concentrations and emission rates of aerial ammonia, nitrous oxide, methane, carbon dioxide, dust and endotoxin in UK broiler and layer houses. *Br. Poult. Sci.* **1997**, *38*, 14–28. [\[CrossRef\]](#) [\[PubMed\]](#)
33. Wheeler, E.F.; Casey, K.D.; Gates, R.S.; Xin, H.; Zajackowski, J.L.; Topper, P.A.; Liang, Y.; Pescatore, A.J. Ammonia emissions from twelve US broiler chicken houses. *Trans. Asae* **2006**, *49*, 1495. [\[CrossRef\]](#)
34. Heber, A.J.; Lim, T.-T.; Ni, J.-Q.; Tao, P.-C.; Schmidt, A.M.; Koziel, J.A.; Hoff, S.J.; Jacobson, L.D.; Zhang, Y.; Baughman, G.B. Quality-assured measurements of animal building emissions: Particulate matter concentrations. *J. Air Waste Manag. Assoc.* **2006**, *56*, 1642–1648. [\[CrossRef\]](#)
35. Heber, A.J.; Ni, J.-Q.; Lim, T.T.; Tao, P.-C.; Schmidt, A.M.; Koziel, J.A.; Beasley, D.B.; Hoff, S.J.; Nicolai, R.E.; Jacobson, L.D. Quality assured measurements of animal building emissions: Gas concentrations. *J. Air Waste Manag. Assoc.* **2006**, *56*, 1472–1483. [\[CrossRef\]](#)
36. Maurer, D.L.; Koziel, J.A.; Bruning, K. Field scale measurement of greenhouse gas emissions from land applied swine manure. *Front. Environ. Sci. Eng.* **2017**, *11*, 1. [\[CrossRef\]](#)
37. Levine, S.Z.; Calvert, J.G. The mechanism of the photooxidation of ammonia. *Chem. Phys. Lett.* **1977**, *46*, 81–84. [\[CrossRef\]](#)
38. Mozzanega, H.; Herrmann, J.M.; Pichat, P. Ammonia oxidation over UV-irradiated titanium dioxide at room temperature. *J. Phys. Chem.* **1979**, *83*, 2251–2255. [\[CrossRef\]](#)
39. Linsebigler, A.L.; Lu, G.; Yates, J.T., Jr. Photocatalysis on TiO₂ surfaces: Principles, mechanisms, and selected results. *Chem. Rev.* **1995**, *95*, 735–758. [\[CrossRef\]](#)
40. Roman, E.; De Segovia, J. Adsorption of ammonia on TiO₂ (001) at room temperature. *Surf. Sci.* **1991**, *251*, 742–746. [\[CrossRef\]](#)
41. Henrich, V.E.; Dresselhaus, G.; Zeiger, H. Chemisorbed phases of H₂O on TiO₂ and SrTiO₃. *Solid State Commun.* **1977**, *24*, 623–626. [\[CrossRef\]](#)
42. Maxime, G.; Amine, A.A.; Abdelkrim, B.; Dominique, W. Removal of gas-phase ammonia and hydrogen sulfide using photocatalysis, nonthermal plasma, and combined plasma and photocatalysis at pilot scale. *Environ. Sci. Pollut. Res.* **2014**, *21*, 13127–13137. [\[CrossRef\]](#) [\[PubMed\]](#)
43. Jeong, M.-G.; Park, E.J.; Seo, H.O.; Kim, K.-D.; Kim, Y.D.; Lim, D.C. Humidity effect on photocatalytic activity of TiO₂ and regeneration of deactivated photocatalysts. *Appl. Surf. Sci.* **2013**, *271*, 164–170. [\[CrossRef\]](#)
44. Seo, H.O.; Park, E.J.; Kim, I.H.; Han, S.W.; Cha, B.J.; Woo, T.G.; Kim, Y.D. Influence of humidity on the photo-catalytic degradation of acetaldehyde over TiO₂ surface under UV light irradiation. *Catal. Today* **2017**, *295*, 102–109. [\[CrossRef\]](#)
45. Boulinguez, B.; Bouzaza, A.; Merabet, S.; Wolbert, D. Photocatalytic degradation of ammonia and butyric acid in plug-flow reactor: Degradation kinetic modeling with contribution of mass transfer. *J. Photochem. Photobiol. A Chem.* **2008**, *200*, 254–261. [\[CrossRef\]](#)
46. Assadi, A.A.; Bouzaza, A.; Wolbert, D. Photocatalytic oxidation of trimethylamine and isovaleraldehyde in an annular reactor: Influence of the mass transfer and the relative humidity. *J. Photochem. Photobiol. A Chem.* **2012**, *236*, 61–69. [\[CrossRef\]](#)
47. Kim, J.S.; Lee, T.K. Effect of humidity on the photocatalytic degradation of trichloroethylene in gas phase over TiO₂ thin films treated by different conditions. *Korean J. Chem. Eng.* **2001**, *18*, 935–940. [\[CrossRef\]](#)

48. Amama, P.B.; Itoh, K.; Murabayashi, M. Photocatalytic degradation of trichloroethylene in dry and humid atmospheres: Role of gas-phase reactions. *J. Mol. Catal. A Chem.* **2004**, *217*, 109–115. [\[CrossRef\]](#)
49. Yao, H.; Feilberg, A. Characterisation of photocatalytic degradation of odorous compounds associated with livestock facilities by means of PTR-MS. *Chem. Eng. J.* **2015**, *277*, 341–351. [\[CrossRef\]](#)
50. Hamdy, M.S. Effect of humidity on the photocatalytic degradation of gaseous hydrocarbons mixture. *Mater. Chem. Phys.* **2017**, *197*, 1–9. [\[CrossRef\]](#)
51. Cant, N.W.; Cole, J.R. Photocatalysis of the reaction between ammonia and nitric oxide on TiO₂ surfaces. *J. Catal.* **1992**, *134*, 317–330. [\[CrossRef\]](#)
52. Wu, H.; Ma, J.; Li, Y.; Zhang, C.; He, H. Photocatalytic oxidation of gaseous ammonia over fluorinated TiO₂ with exposed (0 0 1) facets. *Appl. Catal. B Environ.* **2014**, *152*, 82–87. [\[CrossRef\]](#)
53. Alonso-Tellez, A.; Robert, D.; Keller, N.; Keller, V. A parametric study of the UV-A photocatalytic oxidation of H₂S over TiO₂. *Appl. Catal. B Environ.* **2012**, *115*, 209–218. [\[CrossRef\]](#)
54. Canela, M.C.; Alberici, R.M.; Jardim, W.F. Gas-phase destruction of H₂S using TiO₂/UV-VIS. *J. Photochem.* **1998**, *112*, 73–80. [\[CrossRef\]](#)
55. Yuliaty, L.; Yoshida, H. Photocatalytic conversion of methane. *Chem. Soc. Rev.* **2008**, *37*, 1592–1602. [\[CrossRef\]](#)
56. Fu, Z.; Yang, Q.; Liu, Z.; Chen, F.; Yao, F.; Xie, T.; Zhong, Y.; Wang, D.; Li, J.; Li, X. Photocatalytic conversion of carbon dioxide: From products to design the catalysts. *J. Co2 Util.* **2019**, *34*, 63–73. [\[CrossRef\]](#)
57. Paramasivam, I.; Jha, H.; Liu, N.; Schmuki, P. A review of photocatalysis using self-organized TiO₂ nanotubes and other ordered oxide nanostructures. *Small* **2012**, *8*, 3073–3103. [\[CrossRef\]](#)
58. Tan, S.S.; Zou, L.; Hu, E. Photocatalytic reduction of carbon dioxide into gaseous hydrocarbon using TiO₂ pellets. *Catal. Today* **2006**, *115*, 269–273. [\[CrossRef\]](#)
59. Civiš, S.; Ferus, M.; Knížek, A.; Kubelík, P.; Kavan, L.; Zukalová, M. Photocatalytic transformation of CO₂ to CH₄ and CO on acidic surface of TiO₂ anatase. *Opt. Mater.* **2016**, *56*, 80–83. [\[CrossRef\]](#)
60. Kaiser, J.; Röckmann, T.; Brenninkmeijer, C.A.; Crutzen, P.J. Wavelength dependence of isotope fractionation in N₂O photolysis. *Atmos. Chem. Phys.* **2003**, *3*, 303–313. [\[CrossRef\]](#)
61. Armerding, W.; Comes, F.; Schülke, B. O (1D) quantum yields of ozone photolysis in the UV from 300 nm to its threshold and at 355 nm. *J. Phys. Chem.* **1995**, *99*, 3137–3143. [\[CrossRef\]](#)
62. Kolinko, P.; Kozlov, D. Products distribution during the gas phase photocatalytic oxidation of ammonia over the various titania based photocatalysts. *Appl. Catal. B Environ.* **2009**, *90*, 126–131. [\[CrossRef\]](#)
63. Kočí, K.; Reli, M.; Troppová, I.; Šihor, M.; Kupková, J.; Kustrowski, P.; Praus, P. Photocatalytic decomposition of N₂O over TiO₂/g-C₃N₄ photocatalysts heterojunction. *Appl. Surf. Sci.* **2017**, *396*, 1685–1695. [\[CrossRef\]](#)
64. Wang, H.; Sun, Z.; Li, Q.; Tang, Q.; Wu, Z. Surprisingly advanced CO₂ photocatalytic conversion over thiourea derived g-C₃N₄ with water vapor while introducing 200–420 nm UV light. *J. Co2 Util.* **2016**, *14*, 143–151. [\[CrossRef\]](#)
65. Ohtani, B.; Zhang, S.-W.; Nishimoto, S.-i.; Kagiya, T. Catalytic and photocatalytic decomposition of ozone at room temperature over titanium (IV) oxide. *J. Chem. Soc. Faraday Trans.* **1992**, *88*, 1049–1053. [\[CrossRef\]](#)
66. Černigoj, U.; Štangar, U.L.; Trebše, P. Degradation of neonicotinoid insecticides by different advanced oxidation processes and studying the effect of ozone on TiO₂ photocatalysis. *Appl. Catal. B Environ.* **2007**, *75*, 229–238. [\[CrossRef\]](#)
67. Hernández-Alonso, M.a.D.; Coronado, J.M.; Maira, A.J.; Soria, J.; Loddó, V.; Augugliaro, V. Ozone enhanced activity of aqueous titanium dioxide suspensions for photocatalytic oxidation of free cyanide ions. *Appl. Catal. B Environ.* **2002**, *39*, 257–267. [\[CrossRef\]](#)
68. Pichat, P.; Cermenati, L.; Albini, A.; Mas, D.; Delprat, H.; Guillard, C. Degradation processes of organic compounds over UV-irradiated TiO₂. Effect of ozone. *Res. Chem. Intermed.* **2000**, *26*, 161–170. [\[CrossRef\]](#)
69. Pichat, P.; Disdier, J.; Hoang-Van, C.; Mas, D.; Goutailler, G.; Gaysse, C. Purification/deodorization of indoor air and gaseous effluents by TiO₂ photocatalysis. *Catal. Today* **2000**, *63*, 363–369. [\[CrossRef\]](#)

